Hierarchical theoretical methods for understanding and predicting anisotropic thermal transport release in rocket propellant formulations

Thomas Sewell
MISSOURI SYSTEM, UNIVERSITY OF

12/08/2016
Final Report

Air Force Research Laboratory
AF Office Of Scientific Research (AFOSR)/ RTA1
Arlington, Virginia 22203
Air Force Materiel Command

REPORT DOCUMENTATION PAGE

Form Approved
OMB No. 0704-0188

PLEASE DO NOT RETURN YOUR FORM TO THE ABOVE ORGANIZATION.

1. REPORT DATE *(DD-MM-YYYY)*	2. REPORT TYPE	3. DATES COVERED *(From - To)*
11-28-2016	Final Report	06/15/2014-06/14/2016

4. TITLE AND SUBTITLE
Hierarchical theoretical methods for understanding and predicting anisotropic thermal transport and energy release in rocket propellant formulations

5a. CONTRACT NUMBER

5b. GRANT NUMBER
FA9550-14-1-0091

5c. PROGRAM ELEMENT NUMBER

6. AUTHOR(S)
Thomas D. Sewell
Donald L. Thompson
D. Scott Stewart
Moshe Matalon
Michael Ortiz

5d. PROJECT NUMBER

5e. TASK NUMBER

5f. WORK UNIT NUMBER

7. PERFORMING ORGANIZATION NAME(S) AND ADDRESS(ES)
The Curators of the University of Missouri
Office of Sponsored Program Administration; 115 Business Loop 70W
Mizzou North, Room 501
Columbia, MO 65211-0001

8. PERFORMING ORGANIZATION REPORT NUMBER

9. SPONSORING/MONITORING AGENCY NAME(S) AND ADDRESS(ES)
USAF, AFRL DUNS 143574726
AF OFFICE OF SCIENTIFIC RESEARCH
875 NORTH RANDOLPH STREET, RM 3112
ARLINGTON VA 22203-1954

10. SPONSOR/MONITOR'S ACRONYM(S)
AFOSR

11. SPONSOR/MONITOR'S REPORT NUMBER(S)

12. DISTRIBUTION/AVAILABILITY STATEMENT
DISTRIBUTION A: Distribution approved for public release.

13. SUPPLEMENTARY NOTES

14. ABSTRACT

We summarize a two-year effort to achieve theoretical understanding and predictive capability regarding anisotropic thermal transport and energy release in advanced rocket propellants. The ultimate goal is a practical capability for the a priori design of advanced propellant materials in which structure optimization is used to yield desired energy transport and burn characteristics. Our vision is to exploit anisotropy at three levels:
1) Intrinsic anisotropy at the molecular up to the continuum microscale for pure constituents;
2) Manufactured nano- and microscale anisotropy via manufacture specifications of the composition;
3) Mesoscale anisotropy persistence during physico-chemical structural decomposition, mixing, and reactive processes, templated by item 2).
The overall goal was to combine information from atomic simulations, continuum mesoscopic models of interfaces and interphases, and microstructure-resolved representative volume element simulations. Atomic simulations were carried out for energetic materials to predict thermo-mechanical and transport properties, phase diagrams, and interfacial structure. Mesoscopic models were developed that directly employ ...

15. SUBJECT TERMS
Multiscale methods, Hierarchical structures, Anisotropy, Propellant design, Optimization methods, Gibbs formulation, Molecular dynamics, Mesoscale continuum theory, Thermal transport, HMX, TATB

16. SECURITY CLASSIFICATION OF:			17. LIMITATION OF ABSTRACT	18. NUMBER OF PAGES	19a. NAME OF RESPONSIBLE PERSON
a. REPORT	b. ABSTRACT	c. THIS PAGE			Thomas D. Sewell
U	U	U	UU		19b. TELEPHONE NUMBER *(Include area code)* 573-882-7725

Reset

Standard Form 298 (Rev. 8/98)
Prescribed by ANSI Std. Z39.18
Adobe Professional 7.0

INSTRUCTIONS FOR COMPLETING SF 298

1. REPORT DATE. Full publication date, including day, month, if available. Must cite at least the year and be Year 2000 compliant, e.g. 30-06-1998; xx-06-1998; xx-xx-1998.

2. REPORT TYPE. State the type of report, such as final, technical, interim, memorandum, master's thesis, progress, quarterly, research, special, group study, etc.

3. DATES COVERED. Indicate the time during which the work was performed and the report was written, e.g., Jun 1997 - Jun 1998; 1-10 Jun 1996; May - Nov 1998; Nov 1998.

4. TITLE. Enter title and subtitle with volume number and part number, if applicable. On classified documents, enter the title classification in parentheses.

5a. CONTRACT NUMBER. Enter all contract numbers as they appear in the report, e.g. F33615-86-C-5169.

5b. GRANT NUMBER. Enter all grant numbers as they appear in the report, e.g. AFOSR-82-1234.

5c. PROGRAM ELEMENT NUMBER. Enter all program element numbers as they appear in the report, e.g. 61101A.

5d. PROJECT NUMBER. Enter all project numbers as they appear in the report, e.g. 1F665702D1257; ILIR.

5e. TASK NUMBER. Enter all task numbers as they appear in the report, e.g. 05; RF0330201; T4112.

5f. WORK UNIT NUMBER. Enter all work unit numbers as they appear in the report, e.g. 001; AFAPL30480105.

6. AUTHOR(S). Enter name(s) of person(s) responsible for writing the report, performing the research, or credited with the content of the report. The form of entry is the last name, first name, middle initial, and additional qualifiers separated by commas, e.g. Smith, Richard, J, Jr.

7. PERFORMING ORGANIZATION NAME(S) AND ADDRESS(ES). Self-explanatory.

8. PERFORMING ORGANIZATION REPORT NUMBER. Enter all unique alphanumeric report numbers assigned by the performing organization, e.g. BRL-1234; AFWL-TR-85-4017-Vol-21-PT-2.

9. SPONSORING/MONITORING AGENCY NAME(S) AND ADDRESS(ES). Enter the name and address of the organization(s) financially responsible for and monitoring the work.

10. SPONSOR/MONITOR'S ACRONYM(S). Enter, if available, e.g. BRL, ARDEC, NADC.

11. SPONSOR/MONITOR'S REPORT NUMBER(S). Enter report number as assigned by the sponsoring/ monitoring agency, if available, e.g. BRL-TR-829; -215.

12. DISTRIBUTION/AVAILABILITY STATEMENT. Use agency-mandated availability statements to indicate the public availability or distribution limitations of the report. If additional limitations/ restrictions or special markings are indicated, follow agency authorization procedures, e.g. RD/FRD, PROPIN, ITAR, etc. Include copyright information.

13. SUPPLEMENTARY NOTES. Enter information not included elsewhere such as: prepared in cooperation with; translation of; report supersedes; old edition number, etc.

14. ABSTRACT. A brief (approximately 200 words) factual summary of the most significant information.

15. SUBJECT TERMS. Key words or phrases identifying major concepts in the report.

16. SECURITY CLASSIFICATION. Enter security classification in accordance with security classification regulations, e.g. U, C, S, etc. If this form contains classified information, stamp classification level on the top and bottom of this page.

17. LIMITATION OF ABSTRACT. This block must be completed to assign a distribution limitation to the abstract. Enter UU (Unclassified Unlimited) or SAR (Same as Report). An entry in this block is necessary if the abstract is to be limited.

Air Force Office of Scientific Research, Grant FA9550-14-1-0091

"Hierarchical theoretical methods for understanding and predicting anisotropic thermal transport and energy release in rocket propellant formulation"

Thomas D. Sewell (PI), Professor of Chemistry, University of Missouri-Columbia

Donald L. Thompson (Co-PI), Professor of Chemistry, University of Missouri-Columbia

D. Scott Stewart, Shao Lee Soo Professor of Mechanical Science and Engineering, University of Illinois at Urbana-Champaign (PI of UIUC Subcontract)

Moshe Matalon, Caterpillar Professor of Mechanical Science and Engineering, University of Illinois at Urbana-Champaign

Michael Ortiz, Frank and Ora Lee Marble Professor of Aeronautics and Mechanical Engineering, California Institute of Technology (PI of Caltech Subcontract)

Program Manager Dr. Mitat Birkan, AFOSR/RTE

Final Report for work performed between June 14, 2014 and June 14, 2016

Date Submitted: November 29, 2016

Long-term objective of our research effort: A systematic hierarchical design approach for advanced rocket propellants that exploits intrinsic and engineered anisotropy

The efficacy of new propellants based on hierarchically anisotropic materials depends on structures in the unreacted material, but also on the influence of these structures in the decomposing and burning propellant. Therefore, we think it is useful to think of anisotropy at three levels:

1) Intrinsic anisotropy at the molecular up to the continuum microscale for pure constituents
2) Manufactured nano- and microscale anisotropy that is induced by manufacture specifications of the composition that identifies the material selection, gross stoichiometry, morphology, and constituent placement and orientation
3) Mesoscale anisotropy persistence during the physico-chemical structural decomposition, mixing, and reactive processes, templated by item 2), that results in locally anisotropic effects that appear homogenized at the engineering device-level scale that ultimately defines the performance characteristics of the propellant.

We have longstanding interests in the fundamental physics, chemistry, and engineering required to realize the anisotropy- and hierarchical-design-based approach outlined just above. The goal of our tri-institutional project is *a focused, integrated program of fundamental theoretical and computational research designed to yield understanding and predictive capability regarding anisotropic thermal transport and energy release in advanced rocket propellants.* While fully realizing this goal is not realistically achievable in a three-year effort, the research we are performing will contribute to a longer-term practical capability for the *a priori* design of smart, functional propellant materials based on intelligently designed polymer nanocomposite formulations augmented by non-traditional additives or passivation agents, possibly coupled to external fields.

We believe that the optimal approach is a hierarchical theoretical framework that combines, with as much rigor as possible:

- Fundamental information from atomic-scale simulations
  - Nanoparticles and bulk
  - Interfaces
- Detailed continuum-based mesoscopic models of interfaces and interphases, phase transformations, multi-phase transport, and chemistry
- Explicit microstructure-resolved RVE scale and larger simulations that generate homogenized results induced by mesoscale constituents

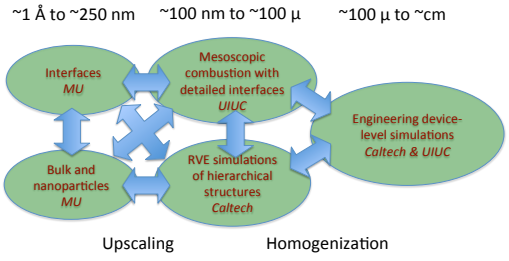

Schematic depiction of nominal spatial scales, physical situations and phenomena, and critical intrascale and scale-bridging connections to be studied.

- Development of approaches that define engineering-scale models for propellant combustion uniquely defined by the hierarchical structures from the molecular, micro-, and mesoscopic models. These engineering-scale models are the ones that can be used to make system performance estimates.

Atomic-scale studies – molecular dynamics (MD) and electronic structure theory – are providing critical knowledge of the details of the physics and chemistry of materials that occur at and in the vicinity of interfaces in advanced propellant formulations. Our studies are resulting in consistent identification, characterization, and quantification of the unit processes of anisotropic mechanical response, transport phenomena, phase stability, and chemical transformation within well-defined (and computationally tractable) physical situations.

We are developing mesoscopic continuum-based models for chemically reactive materials. The general approach taken follows standard methodologies used in the combustion community, but include the complexities associated with anisotropy and heterogeneity that ***must*** be considered to describe nano- and microscale physical processes and their effects on chemistry. Those include consideration of phase changes including solid-state polymorphism and transitions among solid, liquid, and gas; and tracking of key species diagnostic of or critical to the overall reaction kinetics. Multiphase diffusion of species and diffusion of oxidizing and metal ions in oxide melt solutions (often thought to be involved in metal, intermetallic, and thermitic reactions) is being included. The mesoscopic models predict:

- Multiphase decomposition and reaction during chemical energy release at initially separate diffusive/reactive interfaces
- Volumetric reaction and gaseous combustion
- Formalism and constitutive theory used to describe reactants and their products that reflect the underlying material mechanics and physical chemistry of the constituents

We are developing RVE-scale methods for simulating experimentally relevant configurations such as:

- 1-, 2- and 3-D laminates and plies
- Both periodic and stochastic microstructure with designated distributions of materials.

The goal is to simulate a piece of material sufficiently large to yield, in a proper homogenization over the "microscopic" ensemble, statistical distributions of properties that can be used in macro-scale models.

Our research is primarily fundamental with the aim to provide guidance for practical applications. We are focused on establishing tight, direct coupling among the five main elements of the project (see the figure on the preceding page). *The fundamental methods and analysis tools we are developing should be general, so we do not anticipate that they will be successful for one category of material but fail for another.*

University of Missouri-Columbia (MU)

The goals of the MU sub-project are to (1) develop methods and models for atomic-scale simulations of highly anisotropic propellant constituent materials and (2) apply those methods to the careful prediction of the pressure-volume-temperature equation of state, pressure- and temperature-dependent crystal and liquid thermal and transport properties, and fundamental crystal inelastic deformation behaviors (plasticity in the basal plane and the nanoindentation response for oriented crystals). We also studied the melting process and calculated the melting curve $T_{melt}=T_{melt}(P)$ for a range of propellant-relevant pressures. To accomplish these goals we used a combination of molecular dynamics (MD) and molecular mechanics. The focus of our effort is prediction of properties that can be used directly in the larger scale theoretical models under development at the University of Illinois at Urbana-Champaign and the California Institute of Technology, and indeed practically every property we discuss below was chosen for study based on discussions with those collaborators (and, in the second year of this project, has been used by them – Prof. Stewart at UIUC in particular).

MU First Year Summary Comments: Although the energetic crystal 1,3,5-triamino-2,4,6-trinitrobenzene (TATB) is not of practical use as a propellant ingredient, we began our work with this compound as it crystallizes into the lowest symmetry crystal class (triclinic) and exhibits the greatest structural, mechanical, and thermal anisotropy of any energetic compound of which we are aware. Thus, assuming access to a suitable potential energy function with which to perform the simulations, the methods we are developing should be applicable to practically any other energetic compound of interest. We emphasize that our studies under this project are focused on the development of an internally consistent thermo-mechanical description of TATB under "equilibrium" conditions rather than shock loading.

We also performed high-level (essentially benchmark-quality) electronic structure (a.k.a. "quantum chemistry") calculations of proton exchange and transfer in ammonium nitrate (AN) and ammonium perchlorate (AP), and calculations of pathways and energetics for the overall reaction $Al + CO_2 \rightarrow AlO + CO$. Proton transfer is often thought to be an early reaction in the decomposition of inorganic salts such as AN and AP, which are commonly used oxidizers. As an initial stage of developing chemical decomposition schemes for AN and AP, calculations were performed to study the transformation from the stable acid-base pair for isolated formula units to stable ion pairs. In addition to calculations for pure $(AN)_n$ and $(AP)_n$, the effects of NH_3, AlH_3, and BH_3 molecules on cluster acid-base/ion-pair stability were studied. We became interested in the $Al+CO_2$ reaction chemistry both due to its relevance in combustion and because the combined experimental and theoretical descriptions of low-energy $AlCO_2$ complexes appeared to be inconsistent and incomplete. Our work on $Al+CO_2$ should provide a complete, and consistent, description of the various reaction pathways and energetics at the fully optimized CCSD(T) level of theory.

More explicitly, the properties that have been studied, this year and in the first year of the project (which was separated from the current funding increment by a gap of several months), include:

- Force field development for TATB (necessary for MD simulations)

- Anisotropic thermal conductivity in triclinic crystalline TATB as functions of temperature and pressure
- TATB liquid state transport coefficients—thermal conductivity, shear viscosity, and self-diffusion—as functions of temperature and density
- Second-order elastic tensor for TATB for finite temperatures and pressures
- Calculations of plasticity in the TATB basal plane (*i.e.*, in the (001) plane)
- Calculations of nanoindentation of TATB normal to the (100), (010), and (001) crystal surfaces
- Melting point of TATB, T_{melt}, both at normal and elevated pressure (*i.e.*, the melt curve $T_{melt}=T_{melt}(P)$) to 2.0 GPa
- Anisotropic energy transfer from one-dimensional "hot spots" in oriented TATB crystals, including a study of the time and space scales on which energy transport at the nanoscale can be accurately described using the diffusive heat equation (*i.e.*, the continuum heat transfer equation)
- Electronic structure predictions of the transformation from acid-base pairs (*e.g.*, nitric acid and ammonia) to ion pairs (*e.g.*, NH_4^+ and NO_3^-), that is, proton transfer, in small clusters of ammonium nitrate $(AN)_n$ and ammonium perchlorate $(AP)_n$ containing $n \geq 1$ formula units of AN or AP
- Electronic structure calculations of the oxidation of Al by CO_2.
- We also developed and published a method by which the data storage requirements for saving MD simulation trajectories can be drastically reduced, by storing data in a stepwise-uniform fashion in the log(t) domain, in a way that remains consistent with the Shannon-Nyquist sampling theorem.

MU Second Year Summary Comments: In the second year of the project we completed research that carried over from the first year (and from the "original" first year that was funded under a different but intellectually related grant). We also undertook simulations of the mechanical and transport properties for HMX and RDX. These are both propellant-relevant materials, and indeed HMX is a monopropellant. HMX was the focus of the UIUC effort in the second year of the project, and many of the properties that we obtained for HMX are presently in use in the UIUC simulations. More explicitly, the tasks completed and properties that have been studied at MU in the second year include:

- Completion of manuscript preparation or publication for several of the items listed above. The MU reference list (below) has been modified to provide final citations where applicable. Papers that were submitted in the first year but appeared in print during the second year are denoted by an asterisk. Papers that were listed as in preparation at the time of the first-year report but were submitted or published in the second year are treated as second-year publications and thus not denoted by an asterisk.
- Calculation of the complete second-order elastic coefficients for β-HMX on the cold curve for pressures less than 30 GPa. (Manuscript in preparation.)
- Nanoindentation experimentally important planes in β-HMX, (110) and (001). (Work in progress as of this writing.)

- Thermal conduction along the experimentally relevant β-HMX crystal directions (specifically, directions normal to the experimentally important crystal surfaces (110), (011), and (010)).
- Simulations of Kaptiza resistance (i.e., thermal interface resistance) of various energetic crystal binary interfaces including:
    - (001)|(100) in TATB (of interest due to the very high structural anisotropy)
    - (011)|(110) in β-HMX (a grain boundary between the two most prominent interfaces in β-HMX)
    - An α-RDX/β-HMX heterophase interface
    - A nitromethane (100)/(001) grain boundary
    - All of these were in progress at the conclusion of the project.
- Generalized definitions for specifying geometries and calculating grain boundary energetics for simple (i.e., pure twist) and more complicated grain boundaries and heterophase interfaces. (In progress at the end of the project.)

Note: The nanoindentation, thermal conduction, and Kapitza resistance studies listed just above were only possible the benefit of a method published by us very recently [*The Generalized Crystal Cutting Method* (GCCM), Kroonblawd et al., Computer Physics Communications **207**, 232 (2016), supported by a different AFOSR grant] that enables the construction of properly periodic simulation cells for arbitrarily oriented crystal surfaces or oriented homophase or heterophase interfaces.

Most of the efforts mentioned above are described in somewhat greater detail in the following paragraphs.

I. FIRST YEAR WORK, SOME OF WHICH WAS COMPLETED IN YEAR 2

- **Development of a flexible molecule force field for TATB:** We developed[1] potential terms to extend an existing[2] all-atom 1,3,5-triamino-2,4,6-trinitrobenzene (TATB) force field (hereafter, *TATB FF*) to approximately reproduce experimental vibrational spectra and normal modes determined from a density functional theory calculation. The triclinic, layered crystal packing structure for TATB is shown in Fig. 1.[3] The TATB FF has been validated against experimental determinations of the temperature and pressure dependent lattice parameters, heat of sublimation, and bulk modulus.[2,4,5] Many other properties of TATB crystal have never been determined experimentally, due in large part to the difficulties in growing large, high-quality single crystals. The extended force field is currently the best available and most-studied flexible molecule model for TATB and has been used to make numerous predictions for anisotropic thermomechanical properties,[1,2,4-7] the phase diagram,[4,8] transport coefficients,[1,5,6,8] and for up-scaling to parameterize engineering-scale TATB models.[9]

- **An improved force field for high-temperature simulations:** A repulsive intramolecular potential was developed[4] to remedy inaccuracies in the radial distribution function for TATB at temperatures (T) above 750 K predicted by the

TATB FF. This potential was fit to data obtained from constrained geometry optimizations in GAUSSIAN 09 at the M06-2X/6-311G** level. The improved force field predicts realistic intermolecular O-H distances at $T > 750$ K.

- **Reducing data storage costs:** Strategies for non-uniform sampling of simulated relaxation phenomena were developed[10] that can reduce data storage costs by over 90%.

- **Elastic anisotropy and plastic deformation mechanisms:** Complete elastic stiffness tensor of TATB was determined[7] at pressures (P) of 1 atm and 5 GPa by fitting second-degree polynomials to energy-density–strain curves obtained from molecular statics (MS) simulations. Pronounced anisotropy in the elastic response is predicted with significant stiffening under pressure. Plastic deformation in TATB was investigated using Generalized Stacking Fault Energy (GSFE) calculations at pressures of 1 atm and 5 GPa. GSFE calculations, on basal planes, predict that two glide plane types exist for the same glide plane normal. The unstable stacking fault energies on the basal plane are less than 20 mJ/m^2 at 1 atm, indicating easy dislocation glide. A stable stacking fault and a compound twin are predicted to be stable at 1 atm and 5 GPa.

- **Characterization of incipient plasticity from nano-indentation simulations:** Mechanical response of TATB during nano-indentation was investigated[11] using million-atom MD simulations. For the (001) plane, the MD prediction of the elastic part of the force-displacement curve agrees well with predictions from Hertzian contact theory, obtained using the Stroh formalism for anisotropic elasticity (see, Fig. 2(a)). Plastic deformation initiates below the indentation surface, progresses with kinking and delamination of basal planes, and results in extensive pile-up (see, Figs. 2(b) and (c)), with very high temperatures in the vicinity of the indenter (see, Fig. 2(d)). For the (100) plane, MD simulations predict an anomalous, softer response when compared to the prediction from Hertzian contact theory. (Published during second year of project.)

- **Determining the thermal conductivity of defect free TATB crystals:** We made the first predictions of the anisotropic thermal conductivity for TATB single crystals using reverse non-equilibrium molecular dynamics (rNEMD).[1] Our conductivity predictions were determined to be generally insensitive to the details of the intramolecular potential, with all variations predicted to be $\leq$12%.[5] These predictions are similar in magnitude to the available experimental values determined for pressed powder samples. The thermal conductivity for TATB is predicted to be considerably higher and more anisotropic than that for related organic crystalline explosives. Finite-size effects were investigated and found to be minimal,[1,6] indicating that nanoscale thermal transport in TATB crystals may be well-described by continuum theories such as the diffusive heat equation.

- **Understanding conduction in real (defective) TATB crystals:** The impact of dynamic structural transitions and molecular vacancy defects on TATB crystal

thermal conductivity was characterized[6] as a first step toward understanding the conduction properties of real (imperfect) TATB crystals. Approximately linear and anisotropic relationships between molecular vacancy defect density and thermal conductivity are predicted.

- **Characterizing the (*T, P*) dependence of the conductivity:** TATB crystal thermal conductivity was determined as a function of T and P (see Fig. 3).[5] The conductivity is predicted to be proportional to $1/T$, which is consistent with general analytical theories, and anisotropy is predicted to decrease significantly with increasing T. Anisotropic linear increases with increasing P are also predicted. (Published in the second year.)

- **Nanoscale thermal transport in TATB is diffusive:** Molecular dynamics predictions for transient nanoscale hot spot relaxation were compared to continuum-based diffusive heat equation models and reveal such processes are well-described by continuum approaches even at the nanometer length scale (see Fig. 4).[12] (Published in the second year.)

- **Anisotropy in surface-initiated melting:** Surface-initiated melting was investigated[4] using molecular dynamics (MD) simulations for the three principal crystallographic planes exposed to vacuum, with the normal vectors to the planes given by $\boldsymbol{b}\times\boldsymbol{c}$, $\boldsymbol{c}\times\boldsymbol{a}$, and $\boldsymbol{a}\times\boldsymbol{b}$, denoted as (100), (010), and (001), respectively. The nature and extent of disordering of the crystal-vacuum interface depends on the exposed crystallographic face, with the (001) face exhibiting incomplete melting and superheating. This is attributed to the anisotropy of the intermolecular hydrogen bonding and the propensity of the crystal to form stacking faults in directions approximately perpendicular to the (100) and (010) faces. The best estimate of the melting temperature (T_m) at 1 atm for TATB, obtained from surface-initiated melting on the (100) face, is 851 ± 5 K and is 17.7% higher compared to the experimental value of 723 K, obtained using pressed powder pellets.

- **Calculation of the solid-liquid coexistence curve:** Solid-liquid coexistence curve for TATB, at P = 1 atm to 20 kbar, was determined[8] from isobaric-isothermal (NPT) MD simulations of melt in contact with (100) face of the crystal. An upper-bound and a lower-bound for T_m at a particular P is obtained by performing these (solid-liquid coexistence) simulations at multiple T at a particular P and monitoring the volume of the simulation cell as a function of time; the system was deemed to be above or below T_m if the volume increased or decreased, respectively, with time. The solid-liquid coexistence curve is obtained by fitting the Simon-Glatzel equation to (the upper-bound) MD predictions (see, Fig. 5) and is given by:

$$T_m = \left[\frac{(P+6.4808)}{1.6276\times10^{-7}}\right]^{1/2.5892}.$$

Here, T_m is the melting temperature expressed in K and P is the pressure expressed in kbar. We note here that the prediction of T_m at 1 atm, obtained from coexistence simulations, agrees well with the predictions from simulations of surface-initiated melting.

- **Calculation of liquid-phase transport properties for meso-scale simulations:** Shear viscosity (η), self-diffusion coefficient (D), and thermal conductivity (λ) of liquid TATB, at P = 1 atm to 20 kbar and multiple temperatures, are currently being calculated from 4 ns long isochoric-isothermal (NVT) MD simulations.[8] Equilibrium densities for NVT simulations are obtained from independent, 2ns long, NPT simulations. Table I shows the values for η, D, and λ obtained for P = 1 atm. Arrhenius fit of η and D for P = 1 atm (shown in Fig. 6) predicts activation energy of E_η = 7.29 kcal mol^{-1} and E_D = 12.27 kcal mol^{-1}. The thermal conductivity is predicted to be up to 80% lower than for the crystal and linearly decreases with increasing T.

II. SECOND YEAR WORK (EXCLUDING ITEMS MENTIONED ABOVE THAT CARRIED OVER INTO YEAR 2)

β-HMX second-order elastic coefficients on the cold curve: Molecular mechanics energy minimization methods were used to calculation to full second-order elastic coefficients of β-HMX as functions of pressure at 0 K. From these, the Voigt- and Reuss-average isotropic moduli can also be obtained as functions of pressure. The results are shown in Fig. 7.

Nanoindentation in β-HMX: We are using controlled-displacement indentation methods similar to those described above for TATB to study the nanoindentation response for HMX surfaces. As of this writing, the results yield predictions in close agreement with the Hertzian contact model predictions for low levels of displacement but, in contrast to the results for TATB, a lack of the clear load drops that would signify well-defined plastic deformation events. Rather, for the specific case of nanoindentation normal to (110) we find a gradual rolloff behond which the load-displacement curve appears to be flat. This led us to investigate a detail in our simulation protocol, namely whether the indenter was displaced into the sample in a step-wise fashion (using 1.0 Å incremental displacement at 2.5 ps intervals during the simulation) *versus* in a continuous fasion (a very small displacement at every time step of the simulation so as to yield the same 40 m s^{-1} overall indentation rate as used in the stepwise simulations and in our published paper for TATB). We find that the general phenomenon – the smooth rollover to a flat load-displacement curve – is obtained in both cases but (as one might expect) the displacement at which the rollover occurs is higher for the continuous displacement protocol. These results, which are preliminary, are shown in Fig. 8.

Kaptiza resistance: We used the GCCM method to build a (100)/(001) grain boundary interface in TATB within an overall 3-D periodic simulation cell. The grain boundary was oriented normal to the overall simulation cell and a thermal

gradient across the grain boundary was prepared by defining "hot" and "cold" reservoirs in the (001) and (100) regions, respectively, far from the grain boundary. The system was simulated until it reached a steady-fluctuating state afterwhich statistics were accumulated for 4 ns. (See Fig. 9.) This particular grain boundary orientation was chosen because it is essentially the "most anisotropic" one that could exist between two TATB crystals, as is clear from the figure. Despite the pronounced structural anisotropy, the temperature drop across the interface is only 4 ± 9 K (based on linear regression of temperature profiles away from the reservoirs or the interface), yielding a Kapitza resistance of $\sim 10^{-11}$ m^2 K W^{-1}, which is orders of magnitude smaller than values obtained for covalent materials. Our initial explanation for this lack of an effect for the studied case is that the phonon mean free path length in TATB (estimated by us) and other energetic crystals notably including RDX (estimated by others) is of the order of molecular dimensions rather than the very large values characteristic of covalent or ionic materials such as diamond, silicon, or UO_2.

TABLES

Table I. Transport properties of liquid TATB at P = 1 atm.

T (K)	ρ (kg m^{-3})	η (10^{-3} Pa s)	D (10^{-9} m^2 s^{-1})	λ (W m^{-1} K^{-1})
900	1352 (13)	1.262 (0.006)	1.0787 (0.0002)	0.26 (0.01)
950	1303 (13)	1.042 (0.002)	1.608 (0.001)	0.25 (0.01)
1000	1258 (16)	0.860 (0.002)	2.164 (0.001)	0.23 (0.01)
1050	1193 (17)	0.764 (0.006)	2.871(0.002)	0.20 (0.01)
1100	1132 (19)	0.640 (0.006)	3.650 (0.003)	0.190 (0.009)
1150	1046 (23)	0.497 (0.002)	5.020 (0.006)	0.172 (0.008)

FIGURES

Fig. 1.

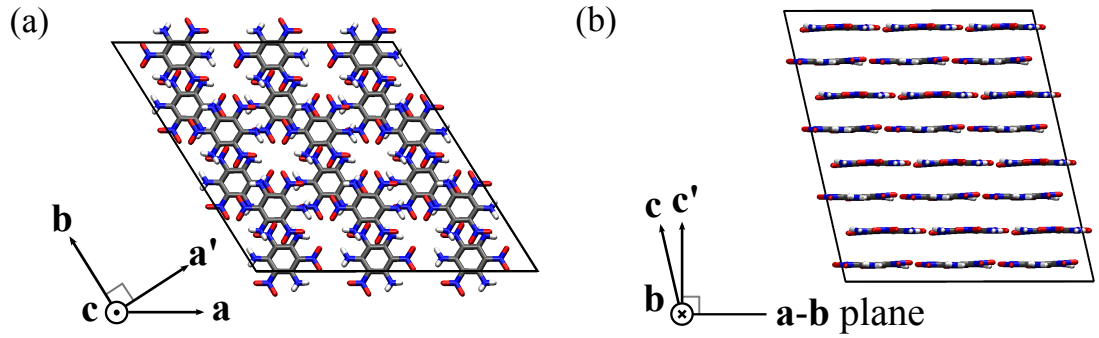

TATB crystal packing structure for a 3**a**×3**b**×4**c** supercell (a) within the planar molecular layers and (b) between the molecular layers. The unit cell contains two molecules and contributes two layers. Due to the triclinic symmetry, the lattice vectors **a**, **b**, and **c** are not mutually orthogonal so vectors **a** and **b** in panel (a) and **c** in panel (b) do not lie exactly within the plane of the page. Thermal conduction is investigated along directions **a'** and **c'**. Atom colors are gray for carbon, blue for nitrogen, red for oxygen, and white for hydrogen.

Fig. 2.

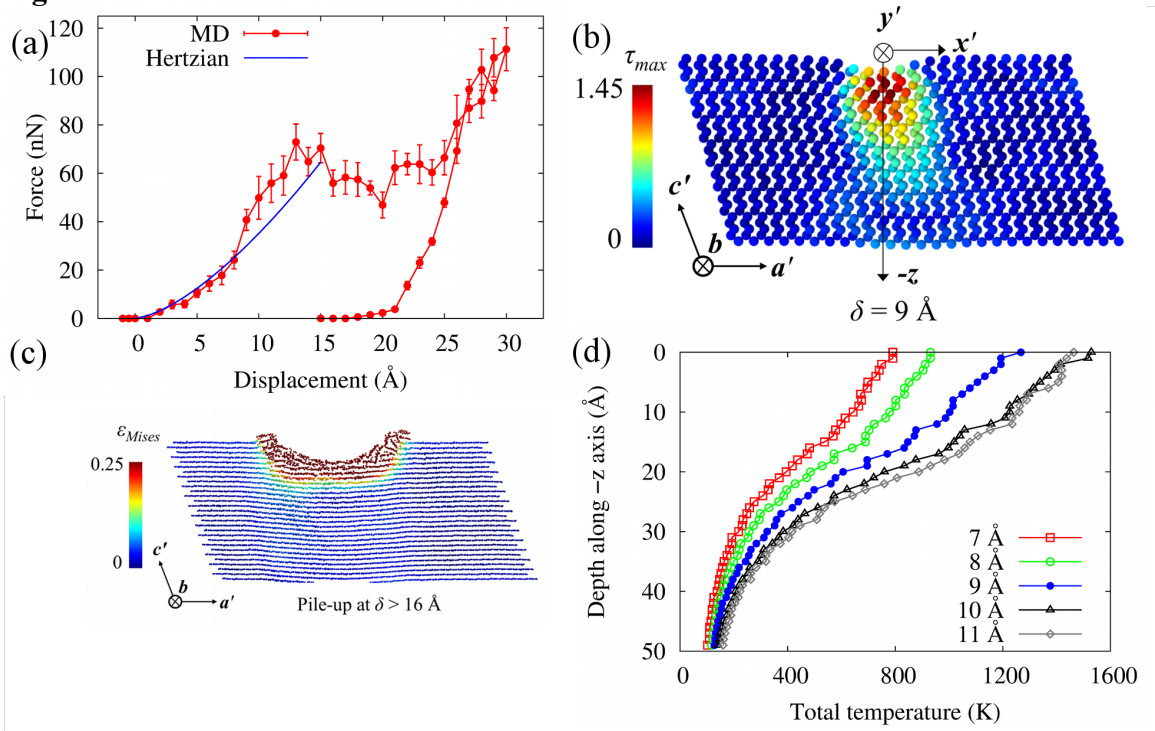

Nanoindentation on the (001) plane of TATB. (a) Force-displacement curve (b) Distribution of maximum shear-stress at $\delta = 9$ Å (c) Pile-up during nanoindentation (d) Locally averaged temperature under the nanoindenter.

Fig. 3.

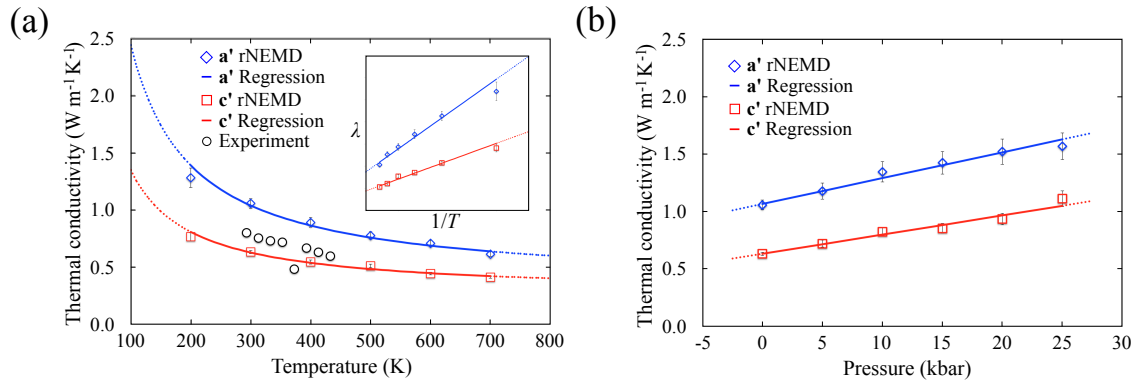

Anisotropic thermal conductivity λ for TATB crystal (a) at P = 1 atm and 200 K $\leq T \leq$ 700 K and (b) at T = 300 K and 1 atm $\leq P \leq$ 25 kbar. Diamond and square symbols are predictions from rNEMD simulations, solid curves are weighted least-squares regressions of rNEMD data fit to $\lambda = m/T + b$ for (a) and to $\lambda = mP + b$ for (b), and dashed curves are extrapolations from the regressions. The inset in panel (a) shows the same results as the main figure but plotted against $1/T$. Experimental values for pressed powder samples[13] are indicated by circle symbols.

Fig. 4.

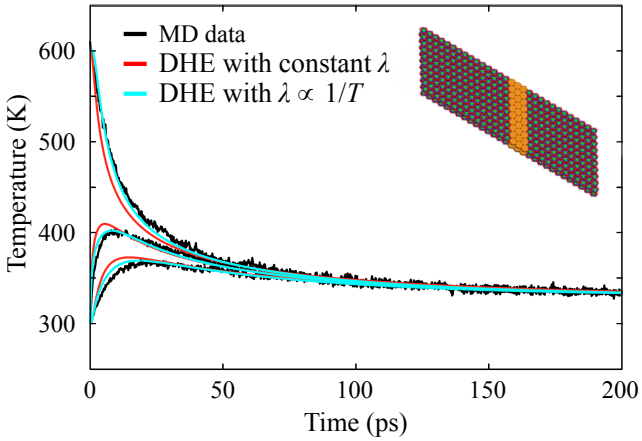

Temperature profiles for selected TATB crystal layers in a relaxation simulation for an idealized 1-dimensional hot spot that is only three unit cells thick. Molecular dynamics predictions (black curves) fit to a constant-conductivity solution (red curves) of the diffusive heat equation (DHE) are in general qualitative agreement. Comparison to a solution with a temperature-dependent conductivity function (cyan curves) highlights the importance of including temperature-dependent parameters in continuum models.

Fig. 5.

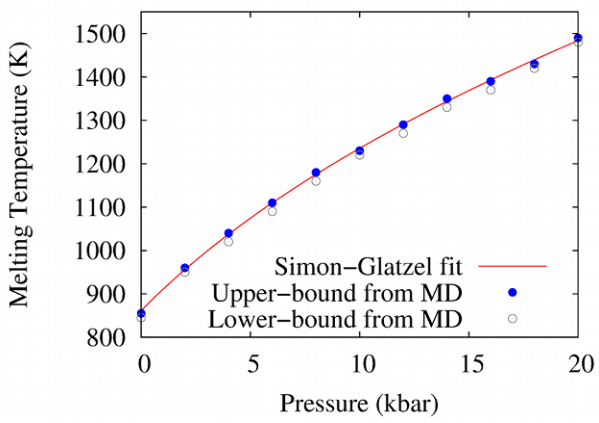

Melt-curve for TATB from solid-liquid coexistence simulations.

Fig. 6.

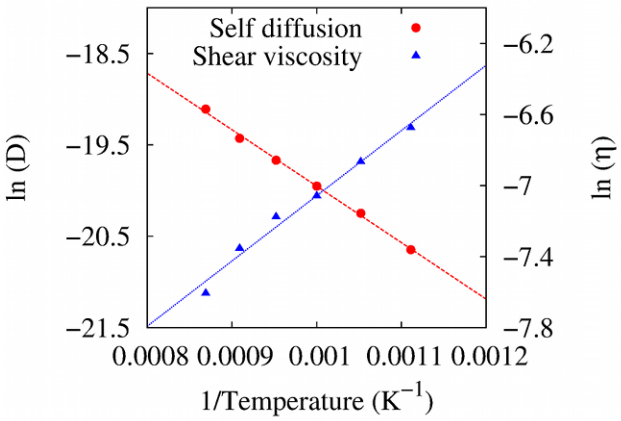

Arrhenius fits to self -diffusion coefficient and shear viscosity of TATB at 1 atm.

Fig. 7.

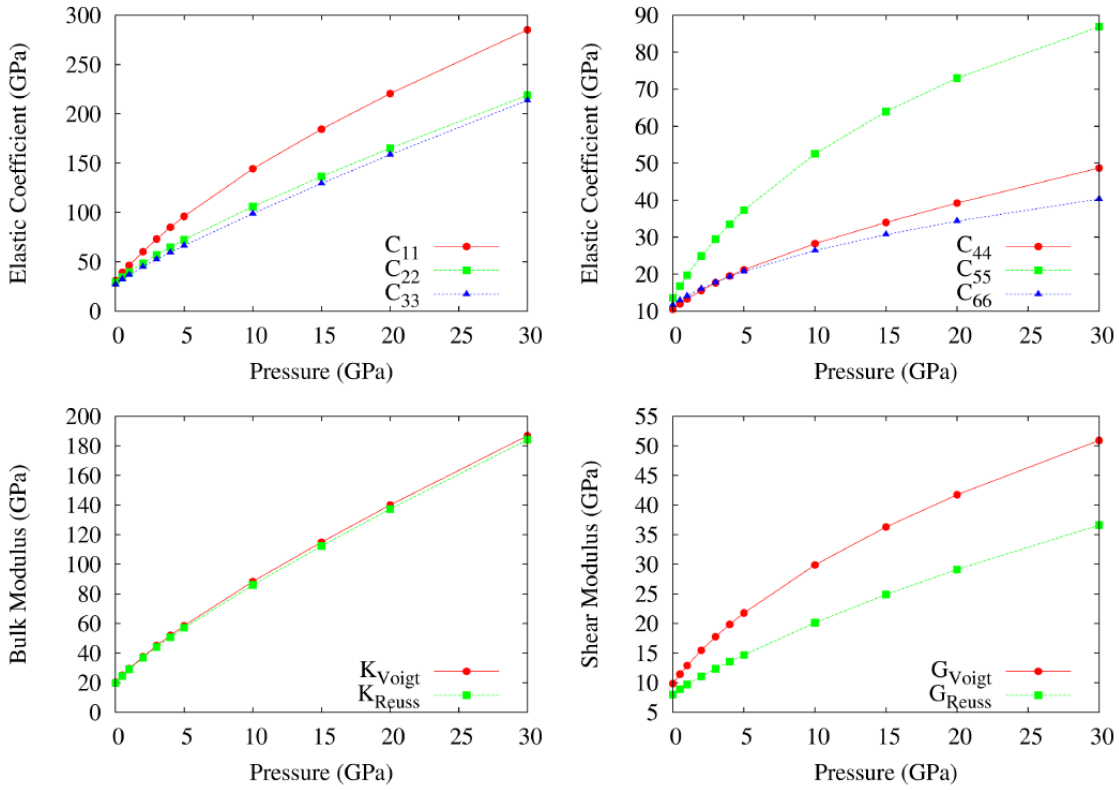

Second-order elastic coefficients and derived isotropic moduli for β-HMX on the cold curve. Only the compressive and pure-shear elements of the tensor are shown. Note the small difference between the Reuss (uniform stress) and Voigt (uniform strain) results for the bulk modulus in contrast to the sizeable difference for the case of the shear modulus.

Fig. 8.

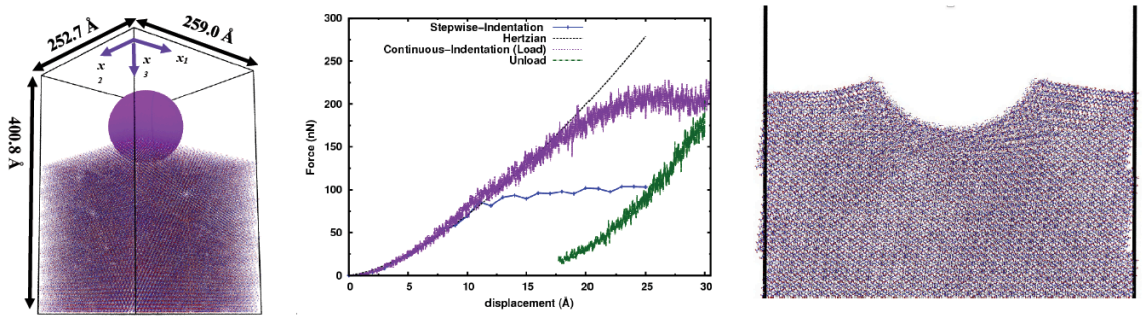

Nanoindentation on (110) planes in β-HMX. Left: Simulation setup. The simulation cell is periodic in the directions normal to the indentation directions. Center: Load-displacement curves for the step-wise indentation (blue solid curve) and continuous indentation (purple curve for loading and green curve for unloading from 30 Å). The Hertzian prediction is shown as the smooth curve. Right: All-atom snapshot of the system for the continuous indenter displacement case for indentation depth 30 Å.

Fig. 9.

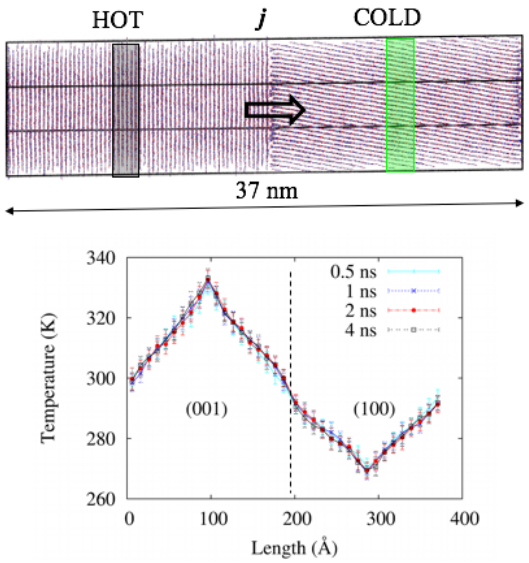

Kapitza resistance across a (001)|(100) grain boundary in TATB. The simulations are 3-D periodic. A hot reservoir in the (001) region and cold reservoir in the (100) region are used to establish a thermal gradient in the system that crosses the grain boundary interface. The Kapitza resistance (thermal interface resistance) is obtained by dividing the temperature jump across the interface (obtained by linear extrapolation of temperature profiles in the respective phases far from the reservoirs and interface) by the thermal flux (which is known exactly). Despite the extremely anisotropic structure at the grain boundary, the Kapitza resistance is predicted to be only ~10-11 m^2 K W^{-1}. This is attributed to the very small phonon mean free path length characteristic of TATB and (apparently) other molecular energetic crystals.

STUDENT AND POSTDOCTORAL RESEARCHER OUTCOMES

- Dr. Jeffrey D. Veals (MU postdoctoral researcher on this project during 2014) was hired as a postdoc at the Army Research Laboratory – Aberdeen Proving Grounds in September 2014. He is now an ARL staff member.
- Dr. Matthew P. Kroonblawd (Ph.D. earned under Prof. Sewell, conferred May 2016) is now a postdoctoral research associate in the Physical and Life Sciences Directorate at Lawrence Livermore National Laboratory.
- Dr. Nithin Mathew (MU postdoctoral researcher on this project 2013-2016) has accepted a postdoctoral research associate position in the Theoretical Division at Los Alamos National Laboratory (start date: late 2016 or early 2017).
- Dr. Shan Jiang (MU postdoctoral researcher on this project 2016) has begun a tenure-track assistant professor position in the Department of Mechanical Engineering at the University of Mississippi ("Ole Miss"; start date: November 2016).

JOURNAL PUBLICATIONS

- *Theoretical determination of anisotropic thermal conductivity for crystalline 1,3,5-triamino-2,4,6-trinitrobenzene (TATB)*, Matthew P. Kroonblawd and Thomas D. Sewell, J. Chem. Phys. **139**, 074503 (2013).
- *Theoretical determination of anisotropic thermal conductivity for initially defect-free and defective TATB single crystals,* Matthew P. Kroonblawd and Thomas D. Sewell, J. Chem. Phys. **141**, 184501 (2014).
- *Generalised stacking fault energies in the basal plane of triclinic molecular crystal 1,3,5-triamino-2,4,6-trinitrobenzene (TATB),* Nithin Mathew and Thomas D. Sewell, Philosophical Magazine **94**, 424 (2015).
- *Strategies for non-uniform sampling of molecular dynamics phase space trajectories of relaxation phenomena*, Matthew P. Kroonblawd and Thomas D. Sewell, Computer Physics Communications **196**, 143 (2015).
- *Anisotropy in surface-initiated melting of the triclinic molecular crystal 1,3,5-triamino-2,4,6-trinitrobenzene: A molecular dynamics study*, Nithin Mathew, Thomas D. Sewell, and Donald L. Thompson, J. Chem. Phys. **143**, 094706 (2015).
- *Predicted anisotropic thermal conductivity for crystalline 1,3,5-triamino-2,4,6-trinitobenzene (TATB): Temperature and pressure dependence and sensitivity to intramolecular force field terms*, Matthew P. Kroonblawd and Thomas D. Sewell, Propellants, Explosives, Pyrotechnics **41**, 502 (2016)
- *Nanoindentation of the triclinic molecular crystal 1,3,5-triamino-2,4,6-trinitrobenzene: A molecular dynamics study*, Nithin Mathew and Thomas D. Sewell, J. Phys. Chem. C **120**, 8266 (2016).
- *Anisotropic relaxation of idealized hot spots in crystalline 1,3,5-triamino-2,4,6-trinitrobenzene (TATB),* Matthew P. Kroonblawd and Thomas D. Sewell, J. Phys. Chem. C **120**, 17214 (2016).

PAPERS IN PREPARATION (meaning a complete manuscript is being finalized):

- *A density functional theory study of Al + CO_2 reactions*, J. D. Veals, R. Chitsazi, Y. Shi, T. D. Sewell, and D. L. Thompson

- *Predicted melt curve and liquid state transport properties of TATB from molecular dynamics simulations*, Nithin Mathew, Matthew P. Kroonblawd, Thomas D. Sewell, and Donald L. Thompson

INVITED PRESENTATIONS

- Matthew P. Kroonblawd, Physical and Life Sciences Directorate, Lawrence Livermore National Laboratory, January 22, 2016
- Nithin Mathew, Theoretical Division, Los Alamos National Laboratory, June 21, 2016
- Thomas S. Sewell, Applied Research Institute, University of Illinois at Urbana-Champaign, July 14, 2014
- Thomas D. Sewell, 2016 Gordon Conference on Energetic Materials, June 7, 2016
- Thomas D. Sewell, Los Alamos National Laboratory MaRIE "" Workshop, Probing Dynamic Processes in Soft Materials Using Advanced Light Sources, July 27, 2016 (post end-date, but covering much of the work accomplished during project lifetime)
- Thomas D. Sewell, 2016 Lawrence Livermore National Laboratory "Mesoscale Modeling of Explosives Initiation Workshop," October 13, 2016 (post end-date, but covering much of the work accomplished during project lifetime)
- Thomas D. Sewell, To be presented at a Los Alamos National Laboratory Workshop "The Behavior, Fabrication and Promise of Intentionally Structured Energetics", to be held 10-12 January 2017 (post end-date, but covering much of the work accomplished during project lifetime)

AWARDS

- Matthew P. Kroonblawd: University of Missouri-Columbia Chemistry Department, Breckenridge/Lyons Award for Outstanding Graduate Research (2016)
- Thomas D. Sewell: University of Missouri-Columbia Fuldner Chemistry Faculty Fellow (2015)
- Thomas D. Sewell: University of Missouri-Columbia Fuldner Chemistry Faculty Fellow (2016)
- Donald L. Thompson: University of Missouri-Columbia Fuldner Chemistry Faculty Fellow (2016)

REFERENCES

[1]M. P. Kroonblawd and T. D. Sewell, J. Chem. Phys. **139**, 074503 (2013).
[2]D. Bedrov, O. Borodin, G. D. Smith, T. D. Sewell, D. M. Dattelbaum, and L. L. Stevens, J. Chem. Phys. **131**, 224703 (2009).
[3]H. H. Cady and A. C. Larson, Acta Crystallogr. **18**, 485 (1965).
[4]N. Mathew, T. D. Sewell, and D. L. Thompson, J. Chem. Phys. **143**, 094706 (2015).
[5] [*] M. P. Kroonblawd and T. D. Sewell, Propell. Explos. Pyro. **41**, 502 (2016).
[6]M. P. Kroonblawd and T. D. Sewell, J. Chem. Phys. **141**, 184501 (2014).
[7]N. Mathew and T. D. Sewell, Philos. Mag. **95**, 424 (2015).
[8]N. Mathew, M. P. Kroonblawd, T. D. Sewell, and D. L. Thompson, "Predicted melt curve and liquid-phase transport properties of TATB," (In preparation, Nov. 2016).
[9]M. P. Kroonblawd, T. D. Sewell, and J.-B. Maillet, J. Chem. Phys. **144**, 064501 (2016).

[10] [*] M. P. Kroonblawd and T. D. Sewell, Comput. Phys. Commun. **196**, 143 (2015).
[11]N. Mathew and T. D. Sewell, J. Phys. Chem. C **120**, 8266 (2016).
[12]M. P. Kroonblawd and T. D. Sewell, J. Phys. Chem. C **120**, 17214 (2016).
[13]R. H. Cornell and G. L. Johnson, "Measuring thermal diffusitivities of high explosives by the flash method," Report No. UCRL-52565, Lawrence Livermore Laboratory, October 1978.

University of Illinois at Urbana-Champaign (UIUC)

1. OVERVIEW OF UIUC SUB-PROJECT

The task objectives state in the original proposal to be carried out by Stewart and Matalon at Illinois were aimed at continuum-based modeling and simulation of multifunctional energetic materials, with the following tasks: 1) Continuum modeling and simulation of microscopic, multi-phase, reactive processes of reactants at the nano- and micro-scale. 2) Design of meso-scale, reactant micro-structure to control and fuel-oxidizer mixing and energy release-rate and 3) System-level and performance evaluation of materials.

A particular emphasis was placed on new models relevant to condensed phase combustion, models that allow for both solid and liquid and gas phase components, phase change, mass diffusion and reaction. The UIUC models are developed to accept inputs from molecular dynamic transport simulations carried out by University of Missouri and other researchers, and suggest new directions for simulations.

At the time of this writing our efforts have completed 2 years of funding and we are starting a 3rd year of partial funding that ends 6/14/2015.

2. UIUC ACTIVITIES DURING FIRST-YEAR PERIOD

A) Continuum Model Development: Multi-component and Mass Diffusion

i) The Gibbs formulation: To describe condensed phase energetic material combustion that occurs in both rocket propellant and liquid rocket propellant ,using physical first principles, Illinois has come up with a new fundamental continuum formulation for the dynamics of multi-component, multi-phase chemically reactive materials. Since the constituent materials used in propellants often are used in explosives, and other energetic materials such as thermite or intermetallic reactive materials, we have been able to carry out model development for this AFOSR effort that has leveraged off of our work from some previous and ongoing projects.

In particular, we note that the Gibbs formulation is a non-equilibrium, continuum thermodynamic formulation *that uses the mass fraction of components (in all phases) as the fundamental configuration variables* instead of previously used order parameters as a marker of the different phase field variables. Kinetic equations that account for the mass creation/destruction and transport of the various components (species) control both phase transformation (melting or evaporation) and chemical reaction. The input to the model includes specifying the various components associated with a given mixture of materials, the equilibrium (Gibbs) potentials for the components, a single component of stress, and a single temperature in the material. Despite the complexity of this model, it enables a proper description of many of the effects one needs to consider in the condensed phase decomposition and reaction processes of propellant materials at the nano and micro-scale, without invoking ad-hoc parameters. The model allows for anisotropic properties of propellant crystallites by invoking an anisotropic potential for the elastic solid. It also

allow for anisotropic thermal conductivities and thermal expansion, the inclusion of state dependent reaction and diffusion kinetics and the use of Arrhenius forms for chemical reaction rates. A significant amount of effort has been expanded in order to validate the model and to ensure it can solve the class of propellant problem of interests.

The general Gibbs formulation was completed this year and is current recorded in a proceedings paper, by Stewart [5], and a longer detailed paper in preparation, that includes many worked examples, see Stewart [8].

ii) Multi-component Diffusion and Kinetics Modeling: One aspect of our effort in this context has been to include realistic multicomponent diffusion, as relevant to the condensed material used in propellants, in order to examine their influence on the burning (diffusion flames), and energy released that takes place at the interface between the fuel and oxidizer. A series of representative problems for condensed phase materials that embrace increasing complexity have been considered, The counterflow diffusion flame (with opposed reactants meeting at a stagnation plane) was used, being a basic configuration that represents the flow due to deformation, from compaction or local heating and thermal expansion processes, in the microscale environment of composite energetic materials. The multi-component diffusion description uses a generalized Fick formulation with coefficient related to the measurable binary diffusivities between two species. A fairly simple depletion form with Arrhenius temperature dependent coefficients is used to describe the reaction rate. Several types of analyses were carried out at increasing levels of complexities (see publications [1] and [3]) and include: an asymptotic analysis valid in the limit of low strain rates (high residence time in the reaction zone), a constant mixture density assumption that simplifies the flow description, diffusion models with equal and unequal molecular weights for the various species, and a full numerical study for finite rate chemistry, composition-dependent density and strain rates extending from low to moderate values. The results suggest that in composite materials there will be a distribution of local reaction sites and local frozen sites that depend on the local strain rate. A related (DTRA) funded effort that focused at the high-temperature titanium/boron forming titanium-boride led to a paper accepted for publication in Combustion and Flame [1] dealing with this particular reaction as a prototype reaction (primarily because of the available kinetic data). Information collected regarding boron properties for modeling is directly relevant to boron additives in propellants. Moreover, the effort established the basic methodologies that are needed to analyze more complex, multi-component kinetics encountered in realistic propellant applications.

a) Numerical verification studies: In addressing the aforementioned studies, we noted that the numerical problems that need to be addressed are extremely stiff, primarily because of the highly temperature-dependent diffusivities and chemical reaction rates, and requires carrying out test problems for verification purposes. In order to establish our basic methods for these very nonlinear, multi-scale problems, we carried out an auxiliary, verification study of ***variable density gaseous counterflow flames*** [3] that had not previously been considered in the literature. This work will be submitted for presentation at the next International Symposium on Combustion scheduled in 2016. We note that

counterflow diffusion flames are prototype flames used in flamelet modeling and relevant to the *non-premixed environment associated with propellant applications*.

This work was carried out simultaneously with that reported in [1] in order to ensure that our numerical tools and methodologies for these highly nonlinear, multi-scale problems are sufficiently robust, as we move to model more realistic and complex kinetics required for propellants. Likewise in [4] Matalon and his student analyzed the structure and dynamics of edge flames in shear flow and the conditions leading *for flame attachment at and liftoff from the base of the injector, or flame blowout.* This knowledge is essential to properly simulate diffusion flames *in the non-premixed environment of propellant applications.*

b) Decomposition schemes for molecular mono-propellants (explosive). Crystallites of nitramines like HMX and RDX have been considered as constituents for advanced propellants due to their high energy density. These materials are both monopropellants and explosives. Their energy release process involves both phase change, (melting) followed by energetic release that occurs from reaction between molecular components that evolve from the thermal decomposition of the crystallites. Fig. 1 shows the comparison of a Gibbs-based continuum simulation (solid lines) of thermal explosion in a constant volume process for RDX, compared with a reactive molecular dynamics simulation (points) that uses ReaxFF (carried out by our UIUC colleague S. Chaudhuri and K Joshi). Although this work was mainly funded by an complementary ONR project, it is mentioned here because it is a basic validation of the Gibbs model and is an essential test of the UIUC modeling strategy.

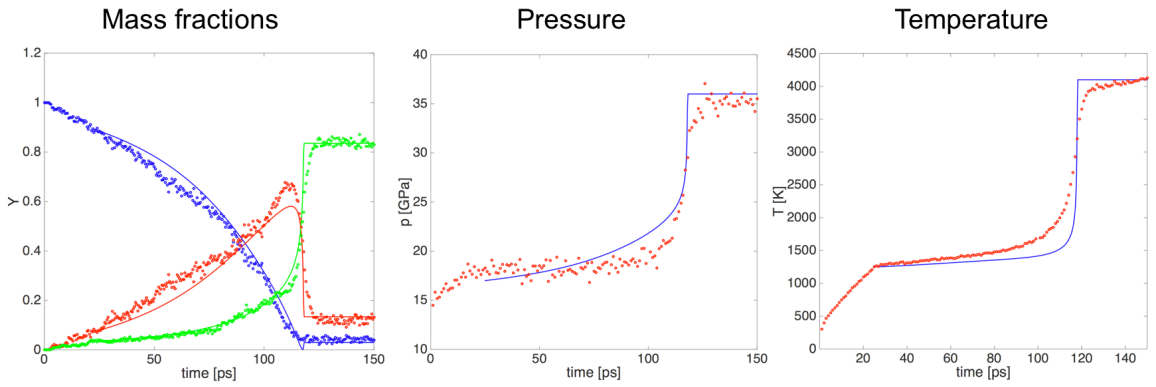

Figure 1. Mass fraction: liquid RDX(blue), intermediate(red), gas phase(green)

In this case we tested the concept of using mass fractions, defined by binning ranges of molecular weights that are observed in the reactive molecular dynamics simulation, and assigning an average molecular weight for that component in a reduced model. A short version of this work will appear as a reference conference proceeding [8], and full length paper [11], will be submitted to the Journal of Chemical Physics. *This work was the first of its kind and shows that we can directly model the results obtained from molecular dynamic simulation by continuum kinetics*. ***This was a test of the basic premise of our Gibbs formulation.***

c) Kinetics scheme and mass diffusion for separated reactants in condensed phase materials: The simple one step global, irreversible reaction F + O --> P is not sufficiently adequate to describe realistic condensed phase combustion processes. The burning of aluminum in the presence of a decomposing oxidizer. like Ammonium Percholorate, is such an example. It requires the consideration of more than just three components (fuel, oxidizer and products), and include aluminum in its solid and liquid phases, the Oxidizer (nominally AP), the decomposition products of AP (such as Perchlorate liquid), and the final products such as aluminum oxide in the liquid and solid phases. The simplest scheme that retains the experimental facts suggests following the evolution of as many as 8 to 12 components. If one considers a one-dimensional unsteady problem, such as the ignition at an interface, or a two-dimensional steady problem such as the counterflow problem, both with reaction occurring at or near a separated reactants material interface, then one must provide a model of mass diffusion for all the 8 to 12 identified components.

In January 2015, at the AFRL Basic Research Review of Computational Research, and Nano-Energetics Review, held at UCLA, D. S. Stewart presented a sketch of an aluminum/AP kinetics scheme for initially separated reactants. Fig. 2 shows the outline of a kinetic scheme currently under consideration by our group.

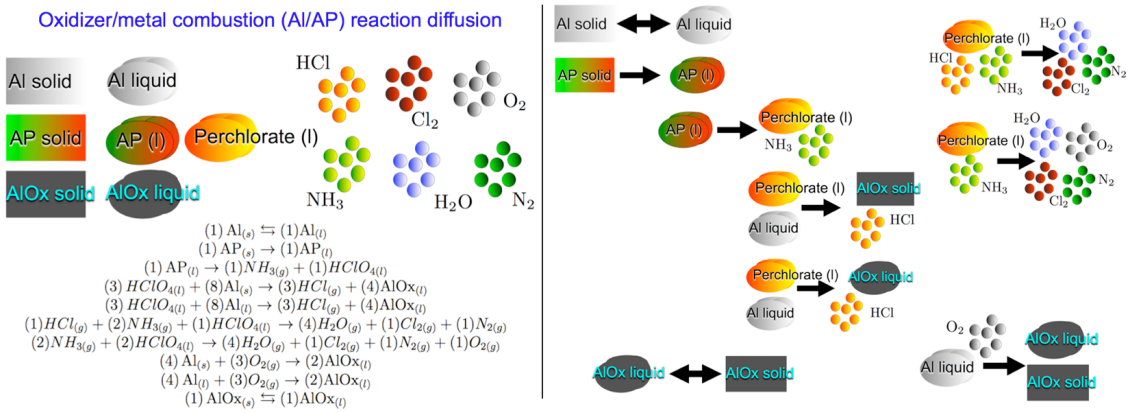

Figure 2. A skeletal kinetics mechanism for AP, aluminum combustion of separated reactants. Eight or more components are required based on work from Guirao and Williams[1]

A take-away point is that one generally requires solid, liquid and gas components for propellant combustion processes in the condensed phase. The kinetic scheme proposed above includes melting of the solid aluminum and solid oxidizer (AP), chemical reaction, as well as the formation of both solid and liquid aluminum oxide products. The analysis of this problem is underway and will build on early work for thermite reaction, [7], [9] that was illustrated for aluminum/copper oxide. The basic premise is similar in that solid reactants are initially separated. For the case of aluminum and copper oxide reactants,

[1]A model of ammonium perchlorate deflagration between 20 and 100 atm , C. Guirao and F. A. WilliamsAIAA Journal, Vol. 9, No. 7 (1971), pp. 1345-1356.

both the aluminum and copper oxide melt, and the liquids react to generate liquid copper and liquid and solid aluminum oxide. And in the same way one must generate a diffusion model that requires at least an effective Fickian diffusion matrix. To carry out such an analysis molecular dynamics simulation can be used to great effect to simplify this model, whereby one can rule out the diffusion of certain components relative to others. The initial work of the Gibbs formulation for the simpler aluminum/copper oxide thermite was invaluable (even though it had 8 components!) in developing schemes to reduce the diffusion matrix to a tractable reduced model. This point was discussed in D. S. Stewart presentation, "Continuum Modeling of Multiphase Energetic Materials at the Nano and Microscale" at the Jan. 2015 UCLA Workshop.

iii) Aluminum particle modeling and electric effects:

It has been hypothesized that small aluminum particles as small as nano-sized particle might provide enhanced heat release when exposed to oxidizer. In particular a 2010 paper by the M. Zacharia group at U. Maryland [2] has suggested that, in the early phase of ignition, at about the temperature at which aluminum melts, that there is an enhanced diffusion mechanism of aluminum cations due to an induced electric charge separation. The charge separation occurs just prior to ignition. They modeled this phenomenon with reactive molecular dynamics, using specifically ReaxFF.

a) Electric on Diffusion Flames: Matalon and his collaborators [2] carried out a precursor study where they analyze ionic transport through the non-premixed reaction zone structure. Two main mechanisms were identified, namely kinetic and body force effects. Kinetic effects are highlighted by a drift velocity that depends on the charge and direction of the electric field such that positively and negatively charged species are drifted in opposing directions, increasing or decreasing the Fickian diffusion velocity. The second mechanism is due to the additional body force highlighted via the "ionic wind" that affects the momentum balance and a Ohmic heating effect that could be positive or negative depending on the flow configuration and direction of the electric field. Due to the imposed symmetry, the ionic wind effect in the droplet problem considered acts only to modify the radial pressure gradient in the combustion field.. Ohmic heating on the other hand was observed to act as a heat source for the droplet setup, leading to a slight increase in flame temperature, enhancement in the burning rate, and extension of the flammability limits.

b) Analysis of a multi-phase material model for an Al/AlOx droplet In order to use the Gibbs formulation to model combustion of nano-sized aluminum particles, Stewart and student K. Lee, developed a model for a spherical aluminum particle with an aluminum oxide cap. Preliminary work established the stress and displacement distributions within the coated aluminum sphere and the transitions in those states as the temperature was increased. These preliminary calculations were reported at the 15th International

[2] On the role of built-in electric fields on the ignition of oxide coated nano-aluminum: Ion mobility versus Fickian diffusion, Brian J. Henz, Takumi Hawa, and Michael R. Zachariah, J. Appl. Phys. **107**, 024901 (2010)

Numerical Combustion meeting, Spring 2015, [14].

This work is the basis for our undergoing analysis of oxidation (burning) of nano, micro-sized aluminum (or metal) particle that occur by diffusional processes. In which case will will add an aluminum cation and and oxygen anions that will diffusive through the oxide layer, and use an approach similar to that Matalon used in [2]. We expect to model Zacharia-group configuration for the particle with the Gibbs formulation, through the end of this grant. And hope to confirm our model results with MD simulations carried out the the Sewell-group at U Missouri or the Chaudhuri group here at UIUC.

Publications and Presentations of the Stewart/Matalon-Group 2014-2015

* - cites AFOSR/RTE support

Peer Reviewed Publications (accepted or submitted)

[1.] * **Diffusion flames in condensed-phase energetic materials**: **Application to Titanium-Boron combustion**, Sushilkumar P. Koundinyan, John B. Bdzil, Moshe Matalon, and D. Scott Stewart, *to appear Combustion and Flame* (2015)

[2.] * **Electric Field Effects in the Presence of Chemi-Ionization on Droplet Burning** A. Patyala , D. Kyritsis , M. Matalon (submitted to Combustion and Flame)

[3.] * **Symmetric counterflow diffusion flames**, S. Koundinyan, M. Matalon, D. S. Stewart, to be submitted to the 36th International *Symposium*

[4.] * **Structure and dynamics of edge flames in the near wake of unequal merging shear flows**, Z. Lu and M. Matalon, submitted to *Combustion Theory and Modelling.*

Peer Reviewed Proceedings Papers

[5.] * ***Modeling reaction fronts of separated condensed phase reactants***, Sushil Koundinyan, M. Matalon, D. S. Stewart, and J. Bdzil, will appear in Shock Compression of Condensed Matter - 2015: Proceedings of the American Physical Society Topical Group on Shock Compression of Condensed Matter; AIP Conf. Proc., Tampa, Florida, June 2015.

[6.] * **A Gibbs Formulation for Reactive Materials with Phase Change** , D. Scott Stewart, will appear in Shock Compression of Condensed Matter - 2015: Proceedings of the American Physical Society Topical Group on Shock Compression of Condensed Matter; AIP Conf. Proc., Tampa, Florida, June 2015.

[7.] * **Modeling the Shock Ignition of a Copper Oxide Aluminum Thermite** , Kibaek Lee, D. S. Stewart, M. Clemenson, N. Glumac, C. Murzyn, will appear in Shock Compression of Condensed Matter - 2015: Proceedings of the American Physical Society

Topical Group on Shock Compression of Condensed Matter; AIP Conf. Proc., Tampa, Florida, June 2015.

[8.] **Mirrored continuum and molecular scale simulations of the ignition of gamma phase RDX,** D. Scott Stewart, Santanu Chaudhuri, Kaushik Joshi. Kiabek Lee, will appear in Shock Compression of Condensed Matter - 2015: Proceedings of the American Physical Society Topical Group on Shock Compression of Condensed Matter; AIP Conf. Proc., Tampa, Florida, June 2015.

Papers in Preparation for Peer Reviewed Publication
(with partial or complete typescript)

[9.] * **Modeling the Shock Ignition of a Copper Oxide Aluminum Thermite**, Kibaek Lee, D. S. Stewart, to be submitted to Journal of Applied Physics

[10.] * **A Gibbs Formulation for Reactive Materials with Phase Change**, D. Scott Stewart, in preparation.

[11.] **Mirrored continuum and molecular scale simulations of the ignition of gamma phase RDX**, D. Scott Stewart, Santanu Chaudhuri, Kaushik Joshi. Kiabek Lee, to be submitted to the Journal of Chemical Physics.

Conference Presentations without Proceedings

[12] * **Compressible mixing of liquid fuels**, Alberto Hernández, Svjetlana Stekovic, D. Scott Stewart and Alexander Wass, 15th International Conference on Numerical Combustion, Avignon, France, April 2015

[13] * **Predicting extinction in condensed phase combustion in a counterflow geometry**, Sushil Koundinyan, M. Matalon, D. S. Stewart, and J. Bdzil, 15th International Conference on Numerical Combustion, Avignon, France, April 2015

[14] * **Analysis of a multi-phase material model for an Al/AlOx droplet**, Kibaek Lee, D. Scott Stewart, 15th International Conference on Numerical Combustion, Avignon, France, April 2015

3. UIUC ACTIVITIES DURING SECOND-YEAR PERIOD

A) *Continuum Model Development*: The Gibbs formulation: Modeling of HMX decomposition.

To describe condensed phase energetic material combustion that occurs in both rocket propellant and liquid rocket propellant, using physical first principles, Illinois developed a new fundamental continuum (Gibbs) formulation for the dynamics of multi-component, multi-phase chemically reactive materials. Since the constituent materials used in propellants often are used in explosives, and other energetic materials such as thermite or intermetallic reactive materials, we have been able to carry out model development for this AFOSR, leveraged off of our work from some previous and ongoing projects. In particular a work recently published in [1], used a Gibbs formulation that and defined a kinetics scheme for nitramine-based energetic materials, that was used modeled decomposition in RDX. The Gibbs formulation faithfully modeled the averages observed in reactive molecular dynamics simulations and thus defined relevant intermediate species and phases.

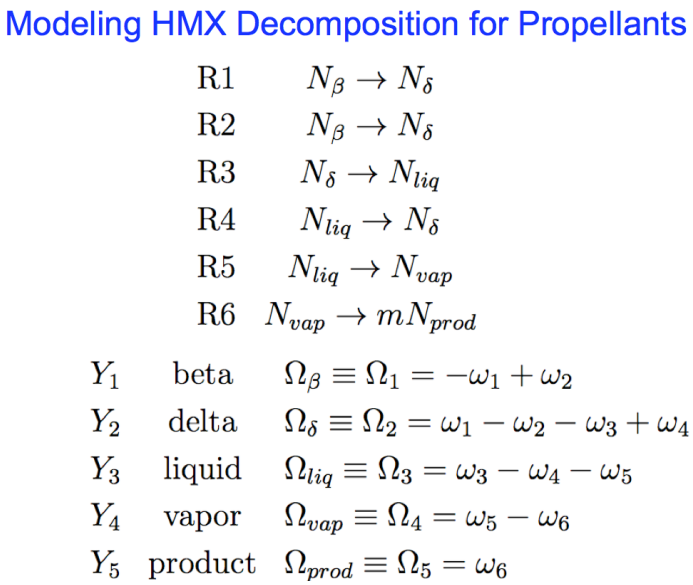

Figure 1. A simplified HMX decomposition scheme for propellants that includes changes from beta to delta solid phase, liquid phase, gas and product gas phase components.

Notably HMX is a constituent used in high performance ballistic missile solid rocket motors. A similar kinetics model was employed, and significantly extended to model a HMX decomposition flame. Figure 1. displays the simplified kinetics and identifies the component used in the model. The UIUC model now includes transport and allows for the progression of a decomposition path, expected to be observed in an HMX monopropellant flame that goes from solid phase through liquid to vapor to burnt product.

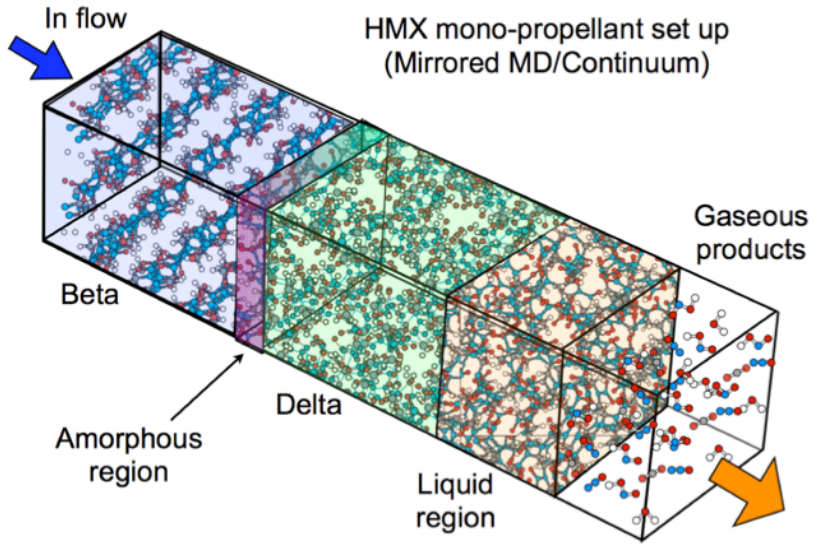

Figure 2. Schematic of the Strand burner configuration for monopropellant burning of HMX, developed in the UM/CIT/UIUC joint effort. The UIUC model developed last year considered the phase shown as basic decomposition steps.

A 1D unsteady model for burning of HMX with dissolved liquids and gases.

Near the end of the work period, UIUC had developed a one-dimensional, but unsteady model, for the burning of HMX. The model had the multiple components discussed above and allows for dissolved liquids and gases in the material mixture. The reduced model allowed one to solve for the thermal and mass fractions and then compute the stress/strain fields. The modeling framework is tractable and will be passed to the CIT (Ortiz)-group if there is additional AFOSR funding for this work. The detailed derivations of the model are, as of yet, unpublished, but they are extensive and the model is complete if not yet validated, [2]. Specifically, the intent is to continue study the properties of this model and generate a still reduced (but tractable) model that can be implemented into the Ortiz computational modeling framework.

A series of 1D, test simulations were carried out using the model. The left edge of a 100-micron slab was raised to constant temperature at the left edge and insulated on the right edge See Fig. 3. Then the simulations showed phase transition, melting and incipient reaction. Therefore we were able to verify the basic integrity of the model and its feasibility. Importantly the thermal expansion in the material is not negligible and significant stress fields can be developed if the material slabs are confined during thermal decomposition. While this is not unexpected we demonstrated that the model could compute/model these affects that are almost never accounted for in other models. Figure 4 shows typical results that illustrate that for a confined slab up to 2 GPa, (20 Kbar) of pressure maybe realized in a confined slab of HMX propellant on the millisecond time scale.

At the time of this writing this work is still in development and will result in publication in the future. This work can be the basis for follow on research supported by AFOSR, and

will be directed to integrated simulations with Cal-Tech.

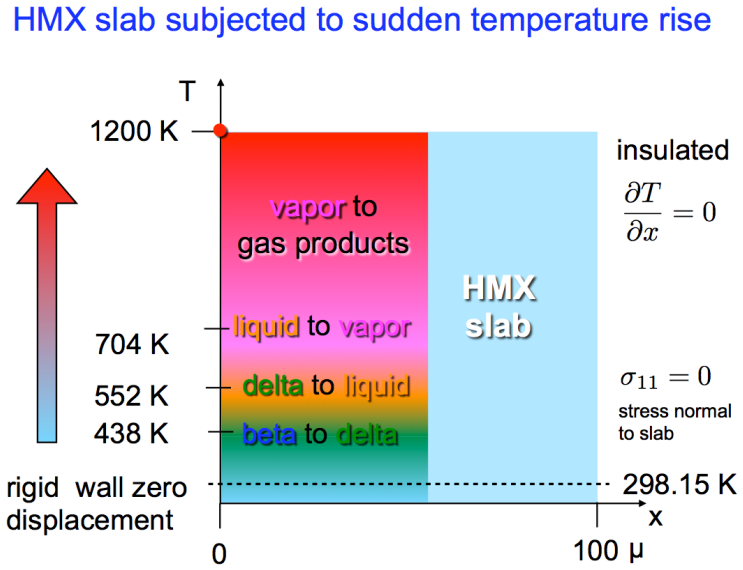

Figure 3. Basic set up for the test problem. The left part of the figure shows the temperatures and the associated phase transitions. The figure is labeled with the boundary conditions imposed on a 100 micron slab with a left edge raised and kept at 1200 Kelvin.

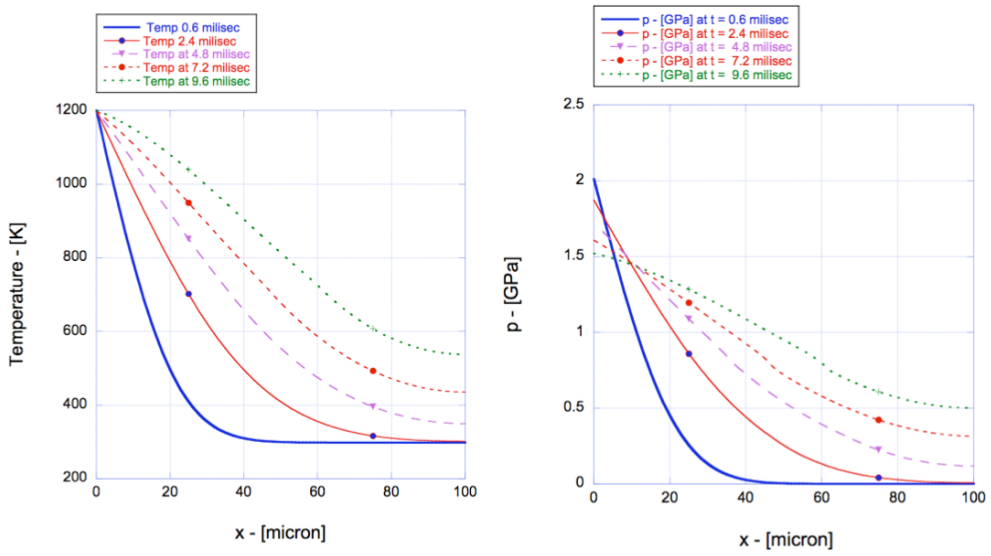

Other Publications and Works Supported by this Grant.

During the last year of the grant, a number of other works were completed and published by Matalon and Stewart and their students at UIUC. The publications that were completed are listed below with attached abstracts that provide a summary of the work. In all cases the work carried out was supported wholly or in part by this grant and cite AFOSR support. These work treat a variety of important issued that include multi-components modeling, thermal transport and electric field variation and their impacts on flames. All these issues are relevant to propellant flame modeling.

Diffusion flames in condensed-phase energetic materials: Application to Titanium–Boron combustion

Combustion and Flame Vol. 162 (2015) pp. 4486–4496

Sushilkumar P. Koundinyan, John B. Bdzil, Moshe Matalon and D. Scott Stewart

The characteristics of a steady diffusion flame that arises at the interfaces of two condensed phase reactant streams that form an opposed counterflow are discussed. We assume that the flow is due to deformation from compaction or local heating and thermal expansion processes in the microscale environment of composite energetic materials. As a representative example of high temperature combustion of metal/intermetallic reactants, the overall reaction of titanium and boron to create titanium diboride products is considered under near isobaric conditions. The multi-component diffusion description uses a generalized Fick formulation with coefficients related to the binary diffusivities defined in the Maxwell–Stefan relations. A fairly simple depletion form with Arrhenius temperature dependent coefficients is used to describe the reaction rate. Several types of analyses are carried out at increasing levels of complexities: an asymptotic analysis valid in the limit of low strain rates (high residence time in the reaction zone), a constant mixture density assumption that simplifies the flow description, diffusion models with equal and unequal molecular weights for the various species, and a full numerical study for finite rate chemistry, composition-dependent density and strain rates extending from low to moderate values. All are found to agree remarkably well in describing the flame structure, the flame temperature and the degree of incomplete combustion. Of particular importance is the determination of a critical strain rate beyond which steady burning may no longer be observed. The analysis has a general character and can be applied to other condensed phase energetic material systems, where reaction and diffusion occur in the presence of flow and material deformation.

Structure and dynamics of edge flames in the near wake of unequal merging shear flows

Combustion Theory and Modelling, Vol. 20, No. 2 (2016) pp. 258–295

Zhanbin Lu and Moshe Matalon

We examine in this study the structure and dynamic properties of an edge flame formed in the near-wake of two initially separated shear flows, one containing fuel and the other oxidiser. A comprehensive study is carried out within the diffusive-thermal framework where the flow field, computed a-priori, is used for the determination of the combustion field. Our focus is on the effects of three controlling parameters: the Damköhler number controlling the overall flow rate, the oxidiser-to-fuel strain rate ratio of the supply streams that determines the extent of oxidiser entrainment towards the mixing zone, and the Lewis number, assumed equal for the fuel and oxidiser, that depends on the mixture composition. Response curves, representing the edge flame standoff distance as a function of Damköhler number, exhibit two distinct shapes: C-shaped and U-shaped curves characterising the response of low and high Lewis number flames, respectively. Stability considerations show that the upper solution branch of the C-shaped response curve is unstable and hence corresponds to physically unrealistic states, but due to heat conduction toward the cold

plate the lower solution branch is always stable. The states forming this solution branch correspond to flame attachment, where the edge flame remains practically attached to the tip of the plate until it is blown off by the flow when the velocity exceeds a critical value. The U-shaped response, on the other hand, consists of equilibrium states that are globally stable. Thus, high Lewis number flames can be always stabilised near the splitter plate, with the edge held stationary or undergoing a back and forth motion, or lifted and stabilised downstream by the flow. Insight into the distinct stabilisation characteristics, exhibited by the different Lewis number cases, is given by examining the relationship between the local flow velocity and the edge propagation speed.

Electric field effects in the presence of chemi-ionization on droplet burning

Combustion and Flame Vol. 164 (2016) pp. 99–110
Advitya Patyal, Dimitrios Kyritsis and Moshe Matalon

The effects of an externally applied electric field on the burning characteristics of a spherically symmetric fuel drop, including the flame structure, flame standoff distance, mass burning rate and flame extinction characteristics of the diffusion flame are studied. A reduced three-step chemical kinetic mechanism that reflects the chemi-ionization process for general hydrocarbon fuels has been proposed to capture the production and destruction of ions inside the flame zone. Due to the imposed symmetry, the effect of the ionic wind is simply to modify the pressure field. Our study thus focuses exclusively on the effects of Ohmic heating and kinetic effects on the burning process. Two distinguished limits of weak and strong field are identified, highlighting the relative strength of the internal charge barrier compared to the externally applied field. For both limits, significantly different charged species distributions are observed. An increase in the mass-burning rate is noticed with increasing the strength of the electric field in both limits, with a small change in flame temperature. Increasing external voltages pushes the flame away from the droplet and causes a strengthening of the flame with a reduction in the extinction Damköhler number.

Temperature-dependent Transport and Thermal-diffusion Effects on Diffusion Flames

Submitted to *Combustion Theory and Modelling*
Joseph E. Hibdon Jr. and Moshe Matalon

The effects of temperature-dependent transport and thermal diffusion, also known as Soret-species transport, on the structure and characteristics of a diffusion flame are studied. The configuration adopted is a planar unstrained diffusion flame, where a uniform flow containing either fuel or oxidizer is directed toward the reaction zone with the oxidizer or fuel diffusing from the opposite boundary against the stream. Included in this discussion is the no-flow case, where the reactants reach the reaction zone purely by diffusion. The model allows for non-unity and distinct Lewis numbers for the fuel and oxidizer and for finite-chemistry effects, covering the entire range of Damköhler numbers, from complete combustion down to extinction. The asymptotic analysis follows the earlier studies on diffusion flames, extended appropriately to accommodate for the temperature-dependent transport coefficients and diffusion fluxes that result from the Soret effect. The results show that both effects lead to a shift in the position of the reaction sheet with a corresponding modification of the stoichiometric flame temperature. Accounting for temperature-dependent transport coefficients lowers the critical Damköhler number, below which flame extinction occurs, thus extending the flammability limits compared to predictions obtained when these coefficients are retained constant. Soret effects have also an effect on these flame characteristics, but the trend depends on the fuel type. The standoff distance of the reaction sheet shifts towards the fuel/oxidizer for “heavy/light fuels”, causing a reduction/increase in flame temperature, respectively. The effect on flame extinction becomes significant only in “heavy fuels” leading to a reduction in the extinction Damköhler number.

Counterflow Diffusion Flames - Numerical Simulations vs Asymptotic

Submitted to *Combustion theory and Modelling*

Sushilkumar P. Koundinyan, John B. Bdzil, Moshe Matalon and D. Scott Stewart

Numerical simulations of counterflow diffusion flames that properly accounts for thermal expansion are presented along with results of the corresponding asymptotic theory for large activation energies. Unlike the idealized constant density case, the variable density asymptotic formulation requires integrating the outer convective-diffusive equations numerically while satisfying the jump relations that mimic the reaction diffusion processes inside the reaction sheet. The numerical implementation of the asymptotic theory, and the numerical simulations of the full governing equations lead to qualitatively identical results, and show good quantitative agreement as well. In particular, the extinction Damköhler number and the flame temperature and position at extinction obtained from both formulations are in good agreement for a wide array of parameters.

References and Supported* Peer Reviewed Publications (accepted and submitted)

[1] Mirrored continuum and molecular scale simulations of the ignition of high-pressure phases of RDX, Kibaek Lee, Kaushik Joshi, Santanu Chaudhuri, and D. Scott Stewart, J. Chem. Phys. 144, 184111 (2016)

[2]* HMX model version1.0, D. Scott Stewart, Unpublished notes, August 8, 2016. A version was presented at the Tri-Services Review, Aug. 2016, Marriot at Key Bridge, Arlington, VA.

[3]* Diffusion flames in condensed-phase energetic materials: Application to Titanium–Boron combustion, Sushilkumar P. Koundinyan, John B. Bdzil, Moshe Matalon and D. Scott Stewart, Combustion and Flame Vol. 162 (2015) pp. 4486–4496

[4]* Structure and dynamics of edge flames in the near wake of unequal merging shear flows, Zhanbin Lu and Moshe Matalon, Combustion Theory and Modelling, Vol. 20, No. 2 (2016) pp. 258–295

[5]* Electric field effects in the presence of chemi-ionization on droplet burning, Advitya Patyal, Dimitrios Kyritsis and Moshe Matalon, Combustion and Flame Vol. 164 (2016) pp. 99–110

[6]* Electric field effects in the presence of chemi-ionization on droplet burning Advitya Patyal, Dimitrios Kyritsis and Moshe Matalon, Combustion and Flame Vol. 164 (2016) pp. 99–110

[7]* Temperature-dependent Transport and Thermal-diffusion Effects on Diffusion Flames, Joseph E. Hibdon Jr. and Moshe Matalon, Submitted to Combustion Theory and Modelling

[8]* Counterflow Diffusion Flames - Numerical Simulations vs Asymptotic Approximation, Sushilkumar P. Koundinyan, Moshe Matalon and D. Scott Stewart, Submitted to Combustion Theory and Modelling

Awards/Honors/Recognitions in the Matalon/Stewart (with a description)

D. Scott Stewart: Program Co-Chair for the 16th International Conference on Numerical Combustion, Orlando, Fl., April 2017

Moshe Matalon: AIAA Fluid Dynamics Award, June 2016.

Invited Talks

Moshe Matalon: Invited talk on "Theoretical considerations in the determination of the laminar burning velocity from laboratory flame configurations", Laminar Burning Velocity Workshop, Rouen, France, March 2015.

Moshe Matalon: Invited plenary talk on "The Hydrodynamic Theory of Premixed Flames: Laminar to Turbulent Propagation", Fifteenth International Conference on Numerical Combustion, Avignon, France, April 2015

Moshe Matalon: Fluid Dynamics Award Lecture on "The Hydrodynamic Theory of Premixed Flames", AIAA AVIATION 2016 Forum and Exposition, June 2016

Stewart/Matalon-Group Collaborations

Defense Reduction Threat Agency, formerly Dr. Suhuti Peiris, Program Manager, recently, ST Enhanced Energetics, AFRL/RW
Dr. David E. Lambert, Chief Scientist, Air Force Research Laboratory Fellow, Munitions Directorate, AFRL/RW, Eglin, AFB, FL
Robert Tompkins, Research Engineer, Raytheon
Dr. Mark Mason, NAVAIR
Dr. Fariba Fahroo, Dr. Arje Nachman, Dr. Mitat Birhkan, Dr. Jennifer Jordan, AFOSR
Dr. John Bdzil, Los Alamos National Laboratory
Dr. Laurence Fried, Lawrence Livermore National Laboratory
Dr. Ronald Brown, Naval Post Graduate School, Monterey CA
Prof. Thomas Sewell, University of Missouri
Prof. William Goddard, Caltech
Dr. Santanu, Chaudhuri, Applied Research Inst., University of Illinois, Urbana, IL

California Institute of Technology

CALTECH ACTIVITIES DURING FIRST-YEAR PERIOD

The work tasked to Caltech is concerned with the development of mesoscale simulations and theory for multi-material and polycrystalline and microstructured materials. Specific subtasks are the generation of useable, verified and validated material descriptions, mixtures and interfacial material interactions that can be directly incorporated into any larger continuum-based computational framework. A primary focus of the work specifically concerns the development of hierarchical theoretical methods for understanding and predicting anisotropic thermal transport and energy release in rocket propellant formulations. An even more specific focus concerns the development of understanding and predictive capability regarding anisotropic thermal transport and energy release in advanced rocket propellants, leading to a practical capability for *a priori* propellant design. Propellants have traditionally been modeled using hydrocodes that neglect entirely the strength of the material. However, recent work (Kroonblawd & Sewell, *J. Chem. Phys*., 2013) has shown that the thermal conductivity of energetic materials such as TATB can be extremely anisotropic, with conductivity contrasts of orders of magnitude depending on transport direction. It seems likely that this extreme anisotropy should in turn result in a strong directional dependence of reaction-front speeds, a phenomenon that appears to be poorly understood at present. This acute sensitivity to local anisotropy in turn raises opportunities for the optimal design of microstructures resulting in enhanced engineering properties of propellants, such as specific impulse, a design tradeoff that also appears to be unexplored at present.
Work at Caltech to date has progressed on two different fronts, described next in turn.

Fundamental understanding of the effect of anisotropy on reaction-front speeds. The essential difficulty in developing such understanding is the multiscale nature of the phenomenon, which includes both atomic level rate-limiting processes, such as thermal vibrations and bond breaking, collisions, coupled to slow processes such as heat and mass transfer, viscosity and complex reactions paths. Indeed, the challenge of performing atomistic full-chemistry simulations over time-scales relevant to macroscopic chemical processes and diffusion-mediated phenomena constitutes a long-standing—yet stubbornly elusive—goal in computational science. For propellants, the time-scale gap is staggering, from thermal vibrations (femptosecond) to device operation (seconds). The spatial-scale gap is equally staggering, from atomic lattice scale (Angstroms) to device dimensions (m). And yet, neither of the limiting scales is sufficient to provide a good-enough handle for material and device design: On one had we wish atomistic realism across within reaction zone in order to account for complex difficult-to-predict reaction paths; on the other hand we wish to make contact with engineering systems and data. The fundamental question is, therefore: How to effect space-time coarse-graining (atoms to device) without introducing spurious physics and without essential loss of information? In effect, we wish for atomistic realism without the need to resolve the length scale of the crystal lattice and the time scale of thermal vibrations.

We have addressed under the auspices of the grant this challenge by developing a theory of *mesodynamics*. The theory is based on a *maximum-entropy* (max-ent) formulation of non-equilibrium statistical mechanics that allows temperature to be defined locally, atom by atom. In this manner, we achieve a statistical description of thermal vibrations away from equilibrium. A system of mesodynamical equations is then defined by projecting the Liouville equation onto the space of max-ent measures. The resulting equations reduce to Hamilton's equations at zero temperature, in

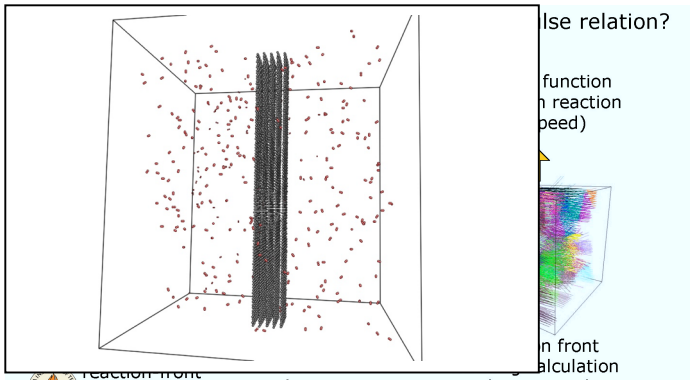

which limit the energy equation becomes redundant. Mesodynamics essentially combines two different descriptions of the motion: deterministic, for the slow components of the motion that are not resolved by the time step; and statistical, for the remaining fast components of the motion, such as thermal vibrations, not resolved by the time step. In calculations, we use *asynchronous integrators* that allow each atom to be updated on its own time step, thus providing various degrees of time resolution depending on local resolution requirements. In addition, the mechanical energy of the fast components of the motion not resolved by the time step is converted locally to heat by recourse to stiffness-proportional damping. For harmonic systems, this form of dissipation damps out preferentially the high-frequency components of the motion while leaving low-frequency components comparatively unchanged. Conversely, when rare events occur, such as hops or collisions, the local time step is decreased in order to provide fine temporal resolution of the events. When such is done, heat is pumped back into the mechanical equations using a random-phase approximation. In this manner, we achieve a fully-resolved, deterministic, description of energetic rare events, such as bond-breaking interactions during chemical reactions, while simultaneously achieving a coarse-grained statistical/ mesodynamical description elsewhere. We have already achieved accelerations of orders-of-magnitude in test cases. At present, we are testing the approach in applications concerned with the oxidation of magnesium and graphite (figure, top left). In addition to providing test cases for the development of the mesodynamics solver, these applications are expected to shed light on the role of thermal anisotropy on reaction-front kinetics.

Development of methods to optimize propellant microstructures. The aim of this effort build on fundamental information from atomic-scale calculations, including orientation-dependent reaction-front speeds, in order to optimize parameterized propellant microstructures of interest, including composites comprising a Polymer binder, oxidizer granules and additives (e.g., NH4ClO4 Composite Propellant, APCP). Key design parameters to be optimized include volume fractions, textures and grain/inclusion morphologies. We connect micromechanical properties to overall propellant performance through front tracking simulations of the passage of reaction fronts through representative volume elements, thus determining effective/macroscopic burning rates. Such effective burning rates are subsequently optimized for maximum specific impulse. To date, we have completed the development and testing of a ray-tracing solver with capability for tracking the passage of reaction fronts through arbitrary locally-anisotropic spatial microstructures (figure, next page). At present, the local reaction-front speed depends on the local anisotropic thermal conductivities through a simple one-step reaction model, but the computational capability is sufficiently general to integrate micromechanical models as they become available. The front tracking calculations are fast enough as to make microstructural optimization feasible. In addition to these computational developments, at present we are attempting to understand the multiscale structure of the problem by analytical means, including closed-form characterization of effective behavior in the sharp-interface limit and in the homogenization limit.

CALTECH ACTIVITIES DURING SECOND-YEAR PERIOD

(BEGINS ON NEXT PAGE)

1 Introduction

The specific impulse delivered by present-day propellants has remained flat since the 1980's. It is clear that radically new propellant preparation paradigms are needed in order to break the current impasse. Recent advances in manufacturing, 3D printing, advanced lithography, nanocomposite materials, vastly expand the design space of propellants and call for a systematic reevaluation of solid propellant technology. Already, adding spheroidal aluminum particles and other metallic phases to propellants is a common technique to increase thrust. However, such approaches beg the question of optimally engineered propellants. A fundamental question in optimal design concerns the geometry and topology of metallic phases resulting in the best possible propellant performance.

We have developed capability that enables topology optimization of complex propellant designs that best balance multiple competing objectives: weight, durability, conductivity, manufacturability and others. We have specifically applied the capability to pilot studies of aluminized composites. We assume that the reaction rate of a propellant is limited by its effective thermal conductivity, as the propellant needs to transport heat to the reaction front in order to sustain the reaction. This ansatz suggests maximizing effective thermal conductivity as one of the optimization objectives. However, thermal conductivity needs to be carefully balanced against competing objectives such as structural integrity and chemistry. In what follow, the multi-objective topology optimization developed to date is showcased by means of test examples. We anticipate that, in subsequent phases of the study, this capability will supply an effective tool for uncovering novel engineered propellant designs with exceptional performance.

2 Review of previous work

Topology optimization with the objective of maximizing heat conduction enables the design of structures that may effectively dissipate or transmit heat generated by a source. This design problem has been explored in detail for a range of applications by various authors. Dede (2009) utilized COMSOL Multiphysics software and a method of moving asymptotes optimizer to investigate a benchmark heat conduction problem involving internal heat generation and a heat sink, resulting in an optimal 'branching' structure.

The author then extended the analysis to a three-terminal heat transfer and fluid flow device. Chen et al. (2010) performed multi-objective topology optimization for finite periodic structures and considered the same benchmark problem in combination with maximizing the stiffness of the structure under mechanical loading. Takezawa et al. (2014) considered topology optimization of a mechanical structure that minimized material volume under both strength and thermal conductivity constraints. Gersborg-Hansen et al. (2006) compared heat conduction topology optimization results modelled by the finite element method and the finite volume method, while Haslinger et al. (2002) used the homogenization method to optimize isotropic bi-material conducting structures.

One particular area of interest has been that of multiple heat load cases, where a number of heat sources act on the structure at different times, locations, and with different heat boundary conditions. Zhuang et al. (2007) used a level set method to explore steady-state heat conduction problems subject to multiple heat load cases with the design objective of constructing an effective transport path for heat dissipation under a given volume constraint. Li et al. (1999) investigated shape and topology design for steady-state heat conduction problems using the ESO method for both single and multiple heat load cases. Design-dependent heat loads, or loads that depend on the material distribution, have been a recent topic of investigation. Iga et al. (2009) considered a total potential energy objective to determine optimally conducting structures subject to design-dependent boundary conditions of heat convection and internal heat generation. Gao et al. (2008) used a modified bidirectional evolutionary structural optimization (BESO) method to explore steady-state heat conduction under both design-independent and design-dependent heat loads.

Heat conduction also plays a role in compliant mechanism topology optimization, where the mechanism relies on the device's own elastic deformation to transfer a motion or force. Sigmund (2001a,b) used the topology optimization method to design thermally and electrothermally driven micro actuators for use in microelectromechanical systems (MEMS). In these systems an heat current is converted to heat which causes thermal strain, which then causes structural deformation. The design objective is to maximize the deformation of a workpiece subject to a constraint on material volume, heat current, out of plane displacement, and also subject to the heat, thermal and elastic equilibrium equations. Yin & Ananthasuresh (2002) presented a design parameterization scheme for topology optimization of MEMS made of multiple

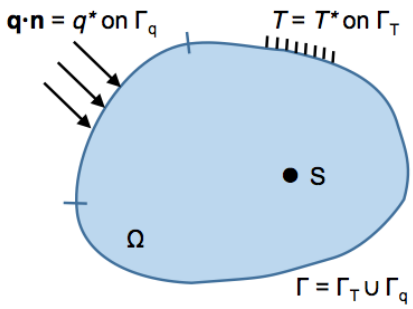

Figure 1: The reference domain

materials and also explored design-dependent boundary conditions, namely heat convection from the device surfaces. Li et al. (2004) designed thermally actuated compliant mechanisms that consider the time-transient effect of heat transfer to produce the localized thermal actuation.

3 Optimization of thermal conductivity

We consider the problem of steady-state heat conduction with no convective heat transfer. Figure 1 depicts a body defined by the volume Ω and outer surface Γ, which is subjected to a prescribed temperature distribution T^* on part of the boundary Γ_T and the normal heat flux q^* is prescribed on the boundary Γ_q.

$$T = T^* \qquad \text{on } \Gamma_T \tag{1}$$

$$\mathbf{q} \cdot \mathbf{n} = q^* \qquad \text{on } \Gamma_q \tag{2}$$

The governing partial differential equation for steady-state heat conduction is

$$\boldsymbol{\nabla}^T (\mathbf{D} \boldsymbol{\nabla} T) + S = 0 \tag{3}$$

or equivalently in it's variational form

$$\int_\Omega \boldsymbol{\nabla} W \cdot (\mathbf{D} \boldsymbol{\nabla} T)\, \mathrm{d}\Omega + \int_{\Gamma_q} W q^*\, \mathrm{d}\Gamma - \int_\Omega W S\, \mathrm{d}\Omega = 0 \tag{4}$$

where $\mathbf{D}$ is the conductivity tensor, S is the internal heat generation and W is a weight function. This governing equation, also known as Poisson's equation, may be used to describe various physics problems by making appropriate parameter substitutions (Donoso & Sigmund, 2004; Huebner et al., 2008).

The design objective of maximizing heat conductance is achieved by minimizing the thermal compliance, and may be expressed in variational form as

$$\min_{T\in\mathbb{T},\rho} : \quad l(T) \tag{5}$$

$$\begin{aligned} \text{subject to} : \quad & a(T,W) = l(W), \quad \text{for all } W \in \mathbb{T}, \\ & \int_\Omega \rho(x)\, d\Omega \le V_f, \\ & \rho(x) \in \{0,1\}, \end{aligned} \tag{6}$$

where

$$a(T,W) = \int_\Omega \nabla W \cdot (\mathbf{D}\nabla T)\, \mathrm{d}\Omega \tag{7}$$

$$l(W) = \int_\Omega WS\, \mathrm{d}\Omega - \int_{\Gamma_q} Wq^*\, \mathrm{d}\Gamma \tag{8}$$

and $\mathbb{T}$ denotes the space of kinematically admissible temperature fields, x is a point within the domain Ω, $\rho(x)$ is the pointwise volume fraction, and V_f is the upper bound on material volume fraction. Using a finite element discretization, the maximum conductance objective may be expressed as

$$\min_{x} : \quad c(\tilde{\mathbf{x}}) = \mathbf{T}(\tilde{\mathbf{x}})^{\mathsf{T}}\mathbf{K}(\tilde{\mathbf{x}})\mathbf{T}(\tilde{\mathbf{x}}) \tag{9}$$

$$\begin{aligned} \text{subject to} : \quad & \mathbf{K}(\tilde{\mathbf{x}})\mathbf{T}(\tilde{\mathbf{x}}) = \mathbf{F} = \mathbf{F}_q + \mathbf{F}_S \\ & \frac{V(\tilde{\mathbf{x}})}{V_0} \le V_f \\ & \mathbf{0} \le \mathbf{x} \le \mathbf{1} \end{aligned}$$

where $\tilde{\mathbf{x}}$ is the vector of physical element densities, $c(\tilde{\mathbf{x}})$ is the compliance, $\mathbf{T}(\tilde{\mathbf{x}})$ is the global temperature vector, $\mathbf{K}(\tilde{\mathbf{x}})$ is the global conductance matrix, $\mathbf{F}$ is the design independent global thermal load vector comprised of both flux and source therms, $V(\tilde{\mathbf{x}}) = \sum_{e=1}^{N} \tilde{x}_e v_e$ is the material volume, V_0 is the design domain volume, V_f is the prescribed volume fraction. The conductance matrix

and thermal load vector are assembled from their element contributions as follows

$$\mathbf{k}_e(\tilde{x}_e) = \int_{\Omega_e} \mathbf{B}_e^T \mathbf{D}_e(\tilde{x}_e)\mathbf{B}_e \, \mathrm{d}\Omega \tag{10}$$

where $\mathbf{B}_e$ contains the shape function derivatives and $\mathbf{D}_e(\tilde{x}_e)$ is the element conductivity matrix comprised of the thermal conductivity values as a function of material density. For an isotropic material, this is given by

$$\mathbf{D}_e(\tilde{x}_e) = d_e(\tilde{x}_e)\mathbf{I} \tag{11}$$

$$\tag{12}$$

where $d_e(\tilde{x}_e)$ is the element's conductivity as a function of element density, and $\mathbf{I}$ is a 3x3 identity matrix. Therefore, the element conductance matrix may be written as

$$\mathbf{k}_e(\tilde{x}_e) = d_e(\tilde{x}_e) \int_{\Omega_e} \mathbf{B}_e^T \mathbf{I} \mathbf{B}_e \, \mathrm{d}\Omega \tag{13}$$

$$= d_e(\tilde{x}_e)\bar{\mathbf{k}}_e \tag{14}$$

where $\bar{\mathbf{k}}_e$ is the element conductance for a unit thermal conductivity. The element thermal load vector is given by

$$\mathbf{f}^e = \mathbf{f}_q^e + \mathbf{f}_s^e \tag{15}$$

$$= -\int_{\Gamma_q^e} \mathbf{N}^{e\,T} q^* \, \mathrm{d}\Gamma + \int_{\Omega^e} \mathbf{N}^{e\,T} S \, \mathrm{d}\Omega \tag{16}$$

Minimizing the compliance minimizes an average measure of temperature, and therefore maximizes the heat heat conduction.

The sensitivity of the thermal compliance with respect to physical element densities $\tilde{x}_e$ is

$$\frac{\partial c(\tilde{\mathbf{x}})}{\partial \tilde{x}_e} = -\mathbf{t}_e(\tilde{x}_e)^T \frac{\partial \mathbf{k}_e(\tilde{x}_e)}{\partial \tilde{x}_e} \mathbf{t}_e(\tilde{x}_e) \tag{17}$$

where the derivative of the element conductance matrix for an isotropic material is

$$\frac{\partial \mathbf{k}_e(\tilde{x}_e)}{\partial \tilde{x}_e} = \frac{\partial d(\tilde{x}_e)}{\partial \tilde{x}_e} \bar{\mathbf{k}}_e \tag{18}$$

$$= \begin{cases} p\tilde{x}_e^{\,p-1}(d^{(1)} - d^{(0)}) \;\; \bar{\mathbf{k}}_e & \text{for SIMP,} \\ \dfrac{1+p}{(1+p(1-\tilde{x}_e))^2}(d^{(1)} - d^{(0)}) \;\; \bar{\mathbf{k}}_e & \text{for RAMP} \end{cases}$$

where p is the penalty parameter and (1) and (0) denote the two material phases. This sensitivity implies that adding conductive material to the design by increasing the element density will decrease the compliance and therefore improve the conductivity of the structure. This is why an upper limit on volume must be prescribed, and this constraint will remain active throughout the optimization process. As with the previous problem formulations, a filtering step converts the above derivative with respect to physical element density to a derivative with respect to the element design variable x_e.

We have tested our implementation with the aid of a classical heat conduction problem studied by numerous authors including Dede (2009), Chen et al. (2010) and Bendsøe & Sigmund (2003). The problem involves determining the optimal material distribution of a 3D structure consisting of a highly conductive material and an insulator, such that thermal conductivity is maximized. The design domain undergoes internal heat generation, with a heat sink at the base of the domain, adiabatic boundaries and a constraint on the maximum allowable volume of the conductive material. A schematic of the problem setup is depicted in Figure 2.

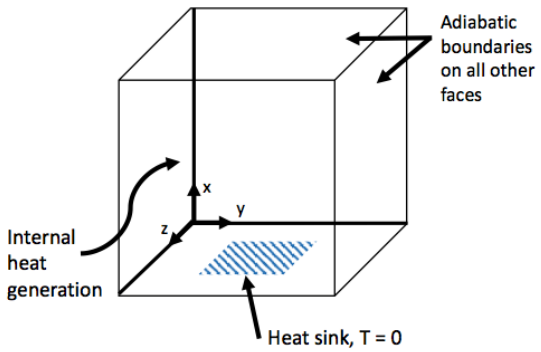

Figure 2: Boundary conditions for the heat conduction test case

Results obtained by both Dede (2009) and Chen et al. (2010) are shown in Figure 3. The optimal topology exhibits a 'branched' structure which fans out towards the boundaries of the domain so that heat is drawn from the domain down to the heat sink.

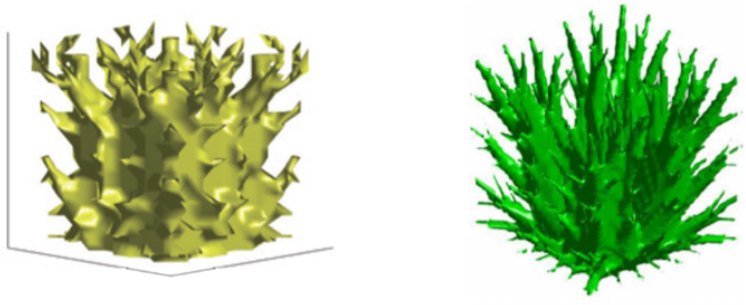

(a) (b)

Figure 3: Optimal structure obtained by (a) Dede (2009), and (b) Chen et al. (2010)

This 3D heat conduction test case is implemented in our topology optimization code using design options and parameter values that would best replicate the problem setup used by previous authors. A cubic design domain with side lengths of 0.2 m is discretized into 50x50x50 cubic elements. We only analyze one quarter of the domain due to the double symmetry of the structure. The desired volume fraction is set to $v_f = 0.30$, and an initial homogeneous distribution of material is prescribed where the element density is set to the given volume fraction. Internal heat generation is applied to all nodes throughout the domain, using an element thermal load vector of $\mathbf{f}_s^e = 0.01^*[1,1,1,1,1,1,1,1]^T$ W. There is s heat sink in a rectangular patch on the bottom face of the domain where the temperature is set to $T = 0°C$. For this problem we consider two materials, both of which exhibit isotropic thermal conductivity. The highly conductive material has a thermal conductivity of $k = 1$ $Wm^{-1}{}^{\circ}C^{-1}$, while the less conductive material has a thermal conductivity of $k = 0.001$ $Wm^{-1}{}^{\circ}C^{-1}$. A SIMP interpolation scheme is used in conjunction with a continuation scheme. The maximum penalty factor is set to $p_{max} = 3$. The algorithm uses a density filter with a filter radius of $r = 0.01$ m or 1.5 element lengths. The method of moving asymptotes is the chosen optimizer. For this problem, we only have design independent loading, therefore the sensitivity is unconditionally negative and the MMA is the best optimizer to use. The GCMMA method will yield virtually identical results

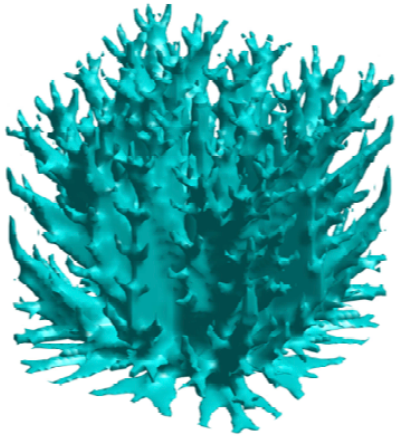

Figure 4: Optimal structure obtained using our topology optimization code

for this particular application, albeit with a greater computational time.

Figure 4 shows the optimized structure obtained using our topology optimization code. It appears that these results are in good agreement with those presented in Figure 3. Iteration history of both the thermal compliance and volume fraction are shown in Figure 5. The compliance converges by approximately 50 iterations while the upper volume fraction limit of $vf = 0.30$ is attained. Possible reasons for slight discrepancies between the three optimized structures include use of different material properties values, thermal load, filter, filter radius, plotting threshold, continuation scheme, solver, and optimization algorithm.

4 Multi-objective optimization

For the specific problem of maximizing heat conduction while ensuring structural integrity in propellants, promising results are expected by combining the maximum structural stiffness and the maximum conduction objective functions. The problem formulation is very similar to that presented by Chen et

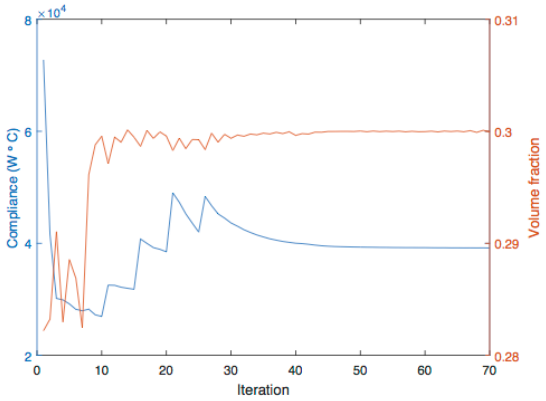

Figure 5: Plot showing thermal compliance and volume fraction vs iterations

al. (2010) and is shown below:

$$\begin{aligned} \min_x : c(\mathbf{x}) &= w_c \frac{\mathbf{\Phi}^T \mathbf{K_c} \mathbf{\Phi}}{C_c^{max}} + w_s \frac{\mathbf{U}^T \mathbf{K_s} \mathbf{U}}{C_s^{max}} \\ \text{subject to} : \frac{V(\mathbf{x})}{V_0} &= f \\ \mathbf{K_c \Phi} &= \mathbf{F_c} \\ \mathbf{K_s U} &= \mathbf{F_s} \\ \mathbf{0} \leq \mathbf{x} &\leq \mathbf{1} \end{aligned} \tag{19}$$

where w_c and w_s are the weighting factors for the maximum conductivity and maximum stiffness objectives ($w_c + w_s = 1$). $\mathbf{K_c}$ and $\mathbf{K_s}$ are the global conductivity and stiffness matrices respectively. The individual objectives are normalized by their maximum values, C_c^{max} and C_c^{max}.

Our computational methodology and implementation of the multi-objective case was verified by replicating the results presented by Chen et al. (2010). Chen et al. developed a topology optimization algorithm for multifunctional 3D finite periodic structures, simultaneously addressing the maximum stiffness and maximum conductivity criteria using a weighted average method. The system setup is very similar to our model where the design objectives are equivalent while the loading and boundary conditions differ, making this example an excellent test case. The mathematical formulation is analogous to Equation 19.

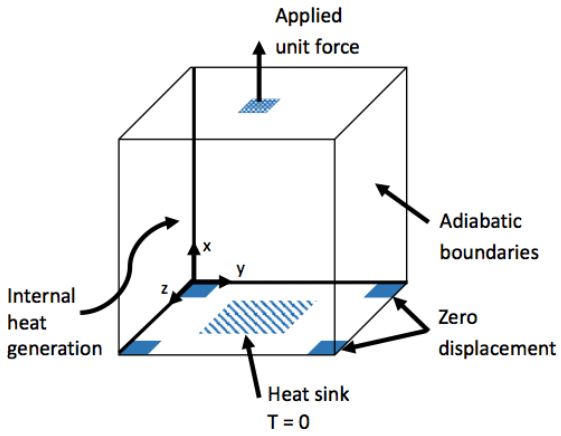

Figure 6: Loading and boundary conditions

The following parameters are used in the optimization algorithm

- Penalty factor, p = 3
- Young's modulus, E = 1
- Poisson's ratio, $\nu = 0.3$
- Conductivity, k = 1
- Volume fraction, $v_f = 0.3$
- Size of domain = 80 x 80 x 80 elements

Zero displacement is prescribed at the bottom four corners of the domain, while a unit force is applied in an upwards direction on the center of the top surface. The design domain is heated evenly at all nodes and a heat sink is located in a square section at the center of the bottom surface (Figure 6).

The results of Chen et al. are provided in Figure 7. The Pareto front shows how the competing design objectives influence the resulting topologies as the weights are varied from $w_s = 0$ (the full conductance case) to $w_s = 1$ (the full stiffness case). When conduction dominates, the optimal design is a doubly-symmetric tree-like configuration with numerous fine twigs, and when

stiffness dominates we obtain a structure with bars connecting the fixed points to the point of loading. The structural topologies obtained using our code are shown in Figure 8, and depict a similar progression of structures as those obtained by Chen et al. Slight discrepancies include the structures in Figure 8c having fewer small branches and differing weight values for visually similar designs. The latter can be attributed to the objectives being normalized by different maximum values, while other causes for the differences include the use of a different filter, filter radius, plotting threshold, continuation scheme and solver, all of which were not specified in the paper. Overall, our results appear in agreement with those presented in Chen et al, thereby verifying our computational methodology and implementation.

References

Bendsøe, M. & Sigmund, O. (2003). *Topology Optimization: Theory, Methods and Applications*. Springer.

Chen, Y., Zhou, S., & Li, Q. (2010). Multiobjective topology optimization for finite periodic structures. *Computers & Structures*, *88*(11âĂŞ12), 806 – 811.

Dede, E. (2009). Multiphysics topology optimization of heat transfer and fluid flow systems. In *Proceedings of the COMSOL Conference*, Boston, MA.

Donoso, A. & Sigmund, O. (2004). Topology optimization of multiple physics problems modelled by poisson's equation. *Latin American Journal of Solids and Structures*, *1*(2), 169–189.

Gao, T., Zhang, W., Zhu, J., Xu, Y., & Bassir, D. (2008). Topology optimization of heat conduction problem involving design-dependent heat load effect. *Finite Elements in Analysis and Design*, *44*(14), 805–813.

Gersborg-Hansen, A., BendsÃŒe, M., & Sigmund, O. (2006). Topology optimization of heat conduction problems using the finite volume method. *Structural and Multidisciplinary Optimization*, *31*(4), 251–259.

Haslinger, J., Hillebrand, A., KÃďrkkÃďinen, T., & Miettinen, M. (2002). Optimization of conducting structures by using the homogenization method. *Structural and Multidisciplinary Optimization*, *24*(2), 125–140.

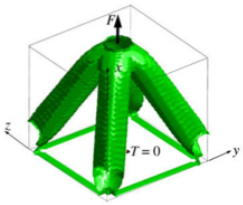

(a) $w_s = 1$

(b) $w_s = 0$

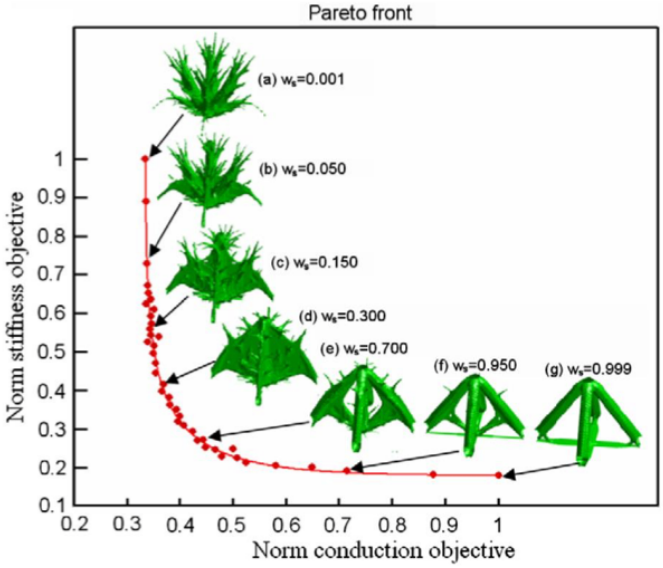

(c) Pareto front and corresponding structural topologies

Figure 7: Topology optimization results produced by Chen et al. (2010).

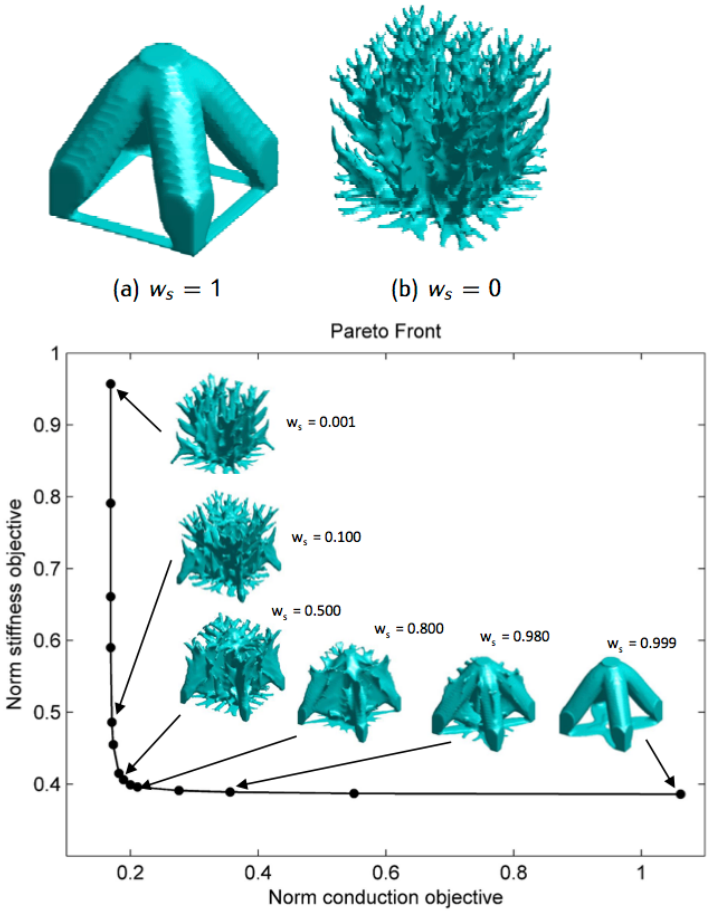

(a) $w_s = 1$ (b) $w_s = 0$

(c) Pareto front and corresponding structural topologies

Figure 8: Topology optimization results produced using our algorithm

Huebner, K. H., Dewhirst, D. L., Smith, D. E., & Byrom, T. G. (2008). *The finite element method for engineers*. John Wiley & Sons.

Iga, A., Nishiwaki, S., Izui, K., & Yoshimura, M. (2009). Topology optimization for thermal conductors considering design-dependent effects, including heat conduction and convection. *International Journal of Heat and Mass Transfer*, *52*(11), 2721–2732.

Li, Q., Steven, G. P., Querin, O. M., & Xie, Y. (1999). Shape and topology design for heat conduction by evolutionary structural optimization. *International Journal of Heat and Mass Transfer*, *42*(17), 3361 – 3371.

Li, Y., Saitou, K., & Kikuchi, N. (2004). Topology optimization of thermally actuated compliant mechanisms considering time-transient effect. *Finite Elements in Analysis and Design*, *40*(11), 1317 – 1331.

Sigmund, O. (2001a). Design of multiphysics actuators using topology optimization âĂŞ part i: One-material structures. *Computer Methods in Applied Mechanics and Engineering*, *190*(49âĂŞ50), 6577 – 6604.

Sigmund, O. (2001b). Design of multiphysics actuators using topology optimization âĂŞ part ii: Two-material structures. *Computer Methods in Applied Mechanics and Engineering*, *190*(49âĂŞ50), 6605 – 6627.

Takezawa, A., Yoon, G. H., Jeong, S. H., Kobashi, M., & Kitamura, M. (2014). Structural topology optimization with strength and heat conduction constraints. *Computer Methods in Applied Mechanics and Engineering*, *276*, 341 – 361.

Yin, L. & Ananthasuresh, G. (2002). A novel topology design scheme for the multi-physics problems of electro-thermally actuated compliant micromechanisms. *Sensors and Actuators A: Physical*, *97âĂŞ98*, 599 – 609. Selected papers from Eurosenors {XV}.

Zhuang, C., Xiong, Z., & Ding, H. (2007). A level set method for topology optimization of heat conduction problem under multiple load cases. *Computer Methods in Applied Mechanics and Engineering*, *196*(4âĂŞ6), 1074 – 1084.

AFOSR Deliverables Submission Survey

Response ID:7287 Data

1.

Report Type

Final Report

Primary Contact Email

Contact email if there is a problem with the report.

SewellT@missouri.edu

Primary Contact Phone Number

Contact phone number if there is a problem with the report

573-882-7725

Organization / Institution name

University of Missouri-Columbia

Grant/Contract Title

The full title of the funded effort.

Hierarchical theoretical methods for understanding and predicting anisotropic thermal transport and energy release in rocket propellant formulation

Grant/Contract Number

AFOSR assigned control number. It must begin with "FA9550" or "F49620" or "FA2386".

FA9550-14-1-0091

Principal Investigator Name

The full name of the principal investigator on the grant or contract.

Thomas D. Sewell

Program Officer

The AFOSR Program Officer currently assigned to the award

Mitat Birkan

Reporting Period Start Date

06/15/2014

Reporting Period End Date

06/14/2016

Abstract

We summarize a two-year effort to achieve theoretical understanding and predictive capability regarding anisotropic thermal transport and energy release in advanced rocket propellants. The ultimate goal is a practical capability for the a priori design of advanced propellant materials in which structure optimization is used to yield desired energy transport and burn characteristics. Our vision is to exploit anisotropy at three levels:
1) Intrinsic anisotropy at the molecular up to the continuum microscale for pure constituents;
2) Manufactured nano- and microscale anisotropy via manufacture specifications of the composition;
3) Mesoscale anisotropy persistence during physico-chemical structural decomposition, mixing, and reactive processes, templated by item 2).

The overall goal was to combine information from atomic simulations, continuum mesoscopic models of interfaces and interphases, and microstructure-resolved representative volume element simulations. Atomic simulations were carried out for energetic materials to predict thermo-mechanical and transport

properties, phase diagrams, and interfacial structure. Mesoscopic models were developed that directly employ output from the atomic-scale simulations. These models were used to predict multiphase decomposition and reaction during chemical energy release at initially separate diffusive/reactive interfaces. Functional optimization methods were used to design potentially realizable microstructures that yield specified physical properties such as maximized thermal conduction or mechanical strength.

Distribution Statement

This is block 12 on the SF298 form.

Distribution A - Approved for Public Release

Explanation for Distribution Statement

If this is not approved for public release, please provide a short explanation. E.g., contains proprietary information.

SF298 Form

Please attach your SF298 form. A blank SF298 can be found here. Please do not password protect or secure the PDF The maximum file size for an SF298 is 50MB.

sf0298FinalReportNov2016.pdf

Upload the Report Document. File must be a PDF. Please do not password protect or secure the PDF . The maximum file size for the Report Document is 50MB.

MU-UIUC-Caltech+AFOSR+Birkan+Annual+(Final)+Report+Nov2016.pdf

Upload a Report Document, if any. The maximum file size for the Report Document is 50MB.

Archival Publications (published) during reporting period:

JOURNAL PUBLICATIONS

• Theoretical determination of anisotropic thermal conductivity for crystalline 1,3,5-triamino-2,4,6-trinitrobenzene (TATB), Matthew P. Kroonblawd and Thomas D.
Sewell, J. Chem. Phys. 139, 074503 (2013).

• Theoretical determination of anisotropic thermal conductivity for initially defect-free and defective TATB single crystals, Matthew P. Kroonblawd and Thomas D. Sewell,
J. Chem. Phys. 141, 184501 (2014).

• Generalised stacking fault energies in the basal plane of triclinic molecular crystal 1,3,5-triamino-2,4,6-rinitrobenzene (TATB), Nithin Mathew and Thomas D. Sewell,
Philosophical Magazine 94, 424 (2015).

• Strategies for non-uniform sampling of molecular dynamics phase space trajectories of relaxation phenomena, Matthew P. Kroonblawd and Thomas D. Sewell, Computer Physics Communications 196, 143 (2015).

• Anisotropy in surface-initiated melting of the triclinic molecular crystal 1,3,5-triamino-2,4,6-trinitrobenzene: A molecular dynamics study, Nithin Mathew, Thomas D. Sewell, and Donald L. Thompson, J. Chem. Phys. 143, 094706 (2015).

• Predicted anisotropic thermal conductivity for crystalline 1,3,5-triamino-2,4,6-trinitobenzene (TATB): Temperature and pressure dependence and sensitivity to
intramolecular force field terms, Matthew P. Kroonblawd and Thomas D. Sewell,Propellants, Explosives, Pyrotechnics 41, 502 (2016)

• Nanoindentation of the triclinic molecular crystal 1,3,5-triamino-2,4,6-trinitrobenzene: A molecular dynamics study, Nithin Mathew and Thomas D. Sewell,J. Phys. Chem. C 120, 8266 (2016).

• Anisotropic relaxation of idealized hot spots in crystalline 1,3,5-triamino-2,4,6-trinitrobenzene (TATB),

Matthew P. Kroonblawd and Thomas D. Sewell, J. Phys.
Chem. C 120, 17214 (2016).

PAPERS IN PREPARATION (meaning a complete manuscript is being finalized):

• A density functional theory study of Al + CO_2 reactions, J. D. Veals, R. Chitsazi, Y. Shi, T. D. Sewell, and D. L. Thompson

• Predicted melt curve and liquid state transport properties of TATB from molecular dynamics simulations, Nithin Mathew, Matthew P. Kroonblawd, Thomas D. Sewell,
and Donald L. Thompson

INVITED PRESENTATIONS
• Matthew P. Kroonblawd, Physical and Life Sciences Directorate, Lawrence Livermore National Laboratory, January 22, 2016
• Nithin Mathew, Theoretical Division, Los Alamos National Laboratory, June 21, 2016
• Thomas S. Sewell, Applied Research Institute, University of Illinois at Urbana-Champaign, July 14, 2014
• Thomas D. Sewell, 2016 Gordon Conference on Energetic Materials, June 7, 2016
• Thomas D. Sewell, Los Alamos National Laboratory MaRIE "" Workshop, Probing Dynamic Processes in Soft Materials Using Advanced Light Sources, July 27, 2016 (post end-date, but covering much of the work accomplished during project lifetime)
• Thomas D. Sewell, 2016 Lawrence Livermore National Laboratory "Mesoscale Modeling of Explosives Initiation Workshop," October 13, 2016 (post end-date, but covering much of the work accomplished during project lifetime)
• Thomas D. Sewell, To be presented at a Los Alamos National Laboratory Workshop "The Behavior, Fabrication and Promise of Intentionally Structured Energetics", to be
held 10-12 January 2017 (post end-date, but covering much of the work accomplished during project lifetime)

New discoveries, inventions, or patent disclosures:
Do you have any discoveries, inventions, or patent disclosures to report for this period?

No

Please describe and include any notable dates

Do you plan to pursue a claim for personal or organizational intellectual property?

Changes in research objectives (if any):

None

Change in AFOSR Program Officer, if any:

None

Extensions granted or milestones slipped, if any:

None

AFOSR LRIR Number

LRIR Title

Reporting Period

Laboratory Task Manager

Program Officer

Research Objectives

Technical Summary

Funding Summary by Cost Category (by FY, $K)

	Starting FY	FY+1	FY+2
Salary			
Equipment/Facilities			
Supplies			
Total			

Report Document

Report Document - Text Analysis

Report Document - Text Analysis

Appendix Documents

2. Thank You

E-mail user

Nov 28, 2016 16:38:25 Success: Email Sent to: SewellT@missouri.edu